学位論文

Development of the pancreas and regeneration process of β cells in medaka

（メダカにおける膵臓の正常発生および β 細胞再生過程の解析）

平成 27 年 12 月博士（理学）申請

東京大学大学院理学系研究科

生物科学専攻

大塚　尭慶

Contents

Abbreviations

- BAC: bacterial artificial chromosome
- db: dorsal bud
- dpa: days post-ablation
- dpf: days post-fertilization
- EGFP: enhanced Green Fluorescent Protein
- hpf: hours post fertilization
- NTR: nitroreductase
- Mtz: metronidazole
- mpf: months post-fertilization
- *pdx1*: pancreatic and duodenal homeobox factor 1
- *ptf1a*: pancreas specific transcription factor 1a
- Tg: transgenic
- vb: ventral bud

Abstract

The pancreas has important roles in food digestion and control of blood glucose level, and is a well-studied organ in mammals because its dysfunction causes serious disorder such as diabetes mellitus and pancreatic cancer. On the other hand, basic information about fish pancreas is still very limited, although it shows a high ability to regenerate lost tissue.

In Chapter 1, I addressed conserved and unique features of development of the fish pancreas by performing extensive analyses of the normal development of the pancreas in medaka embryos and adults using *pdx1*- and *ptf1a*-transgenic medaka, *in situ* hybridization, and immunohistochemistry. A double transgenic (Tg) fish produced in the present study enabled me to visualize the development of endocrine (*pdx1* +) and exocrine (*ptf1a* +) parts simultaneously in living fishes. Like other vertebrates, the medaka pancreas develops as two (dorsal and ventral) buds in the anterior gut tube, which soon fuse into a single anlagen. The double Tg fish demonstrated that the differential property between the two buds is already established at the initial phase of bud development as indicated by strong *pdx1* expression in the dorsal one –it later forms simple "principal islet". Using this Tg fish, I examined the gross morphology and the structure of adult pancreas and revealed unique characters of medaka pancreas such as broad and multiple connections with the gut tube along the anterior-posterior axis and the presence of "secondary islets" that only exists in teleosts.

In Chapter 2, to elucidate the regenerative capacity of pancreatic β cells in

medaka, I generated transgenic lines, in which β cells are specifically ablated by the Nitroreductase (NTR)/ Metronidazole (Mtz) system. I examined β cell regeneration at embryonic and adult stages after specific ablation of β cells and revealed that medaka can regenerate their lost β cells at least at embryonic stages. Furthermore, I found that the teleost-specific secondary islet has an interesting feature that its size changes in response to physiological conditions as indicated by increased size after β cell ablation in the principal islet. I therefore suggest that medaka can be an attractive model for the study of β cell regeneration.

General introduction

The vertebrate pancreas is a bifunctional organ that contains both exocrine and endocrine components and has been the subject of intense investigation because of its essential physiological roles in food digestion and glucose metabolism, and two major human disorders, diabetes mellitus and pancreatic cancer. The endocrine component releases various hormones into the bloodstream for mainly glucose homeostasis. Endocrine cells form clusters, called 'islets', containing at least five specific hormone-producing cells, insulin-producing β cells, glucagon-producing α cells, somatostatin-producing δ cells, pancreatic polypeptide-producing PP cells and ghrelin-producing ε cells (Upchurch *et al.*, 1994, Wierup *et al.*, 2002). The exocrine component, which constitutes the majority of the organ, consists of acinar and duct cells. The acinar cells produce digestive enzymes, such as trypsin, amylase, elastase, and carboxypeptidase A, which are transported into the digestive tract through an elaborate network of ducts (Fig. 1).

The morphogenesis of pancreas during early development has been well characterized in vertebrate models. In amniotes, the pancreas arises from the foregut endoderm as two buds arise from the dorsal and ventral sides of the duodenum (dorsal and ventral buds), which will later fuse to form a single anlage (Guz *et al.*, 1995, Jonsson *et al.*, 1994, Offield *et al.*, 1996). Furthermore, a gene regulatory network has been elucidated in detail, including key transcription factors and signaling molecules essential for pancreatic development (Jensen, 2004, Ben-Othman *et al.*, 2013, Zaret &

Grompe, 2008). Among those factors, pancreatic and duodenal homeobox factor 1 (Pdx1) and pancreas specific transcription factor-1a (Ptf1a/p48) are most crucial in early steps of pancreatic development. They are co-expressed in multipotent progenitor cells and have distinct but interdependent functions in maintenance and specification of the progenitor cells that give rise to endocrine and exocrine cells (Burlison *et al.*, 2008). Later in development, Pdx1 is exclusively maintained in β cells and regulates the expression of insulin as well as other genes required for the function of mature β cells (Chakrabarti *et al.*, 2002). Ptf1a, on the other hand, becomes restricted to the acinar cell lineage and activates exocrine differentiation (Krapp *et al.*, 1998). A larger number of transcription factors have been identified as core regulators of islet cell differentiation, and those include *nkx6.1*, *nkx6.2*, *nkx2.2* and *islet1*. In particular, *islet1* is the first gene identified from β cells and well characterized, which directly regulates *insulin* expression (Karlsson *et al.*, 1990, Ahlgren *et al.*, 1997); it is known to be required for the maturation, proliferation of entire endocrine cells (Du *et al.*, 2009). The gene regulatory network in pancreatic development is summarized in Fig. 2.

Insulin, produced by β cells, is the only hormone that decreases a blood glucose level in our body, and thus dysfunction of β cells results in hyperglycemia and diabetes. Today, most diabetic patients need daily insulin injections. Transplantation of isolated islets is still problematic due to shortage of the donors (Ridgway *et al.*, 2010). One possible solution is transplantation of insulin-producing cells derived from embryonic stem (ES) cells or induced pluripotent stem (iPS) cells (Rood *et al.*, 2006, Tateishi *et al.*, 2008). However, despite accumulated knowledge on the molecular

pathways underlying normal and disturbed pancreatic development (Ben-Othman *et al.*, 2013), we still do not know how to make such pluripotent cells that have abilities to exclusively differentiate into fully functional β cells.

The other possible solution is β cell regeneration and thereby recovery of its function. In general, severely damaged mammalian tissues fail to fully regenerate, although newborn mice tissues temporarily retain the regenerative capacity (Redd *et al.*, 2004). In normal conditions of adult mammalian pancreas, a β cell mass is maintained by self-duplication rather than stem cell differentiation (Dor *et al.*, 2004), and it has been shown that the rate of β cell proliferation is very slow with a long life span (Teta *et al.*, 2005). The adult pancreatic cell mass is determined during embryogenesis. The early endocrine cells aggregate, and its size predetermines the final size of the islets (Desgraz & Herrera, 2009). Many studies have shown that adult pancreas have an ability to generate new β cells when β cells are injured (Desgraz *et al.*, 2011). However, these newly formed β cells do not proliferate sufficiently and as a result, fail to achieve full recovery (Guz *et al.*, 2001, Peshavaria *et al.*, 2006). Thus, the adult mammalian β cells have a very limited capacity under natural conditions.

The morphology of fish pancreas is unique compared with that of other vertebrates. In cartilaginous fish, the pancreas consists of compact organ, which contains both exocrine and endocrine components (Epple & Brinn, 1975) as in other vertebrates. On the other hand, in teleost, a compact pancreas is found only in a few species including eels, catfish, and lungfish (Harder, 1975). Instead, most species of fish have an exocrine pancreatic tissue that is diffusely located around the intestine, but

its exact structure has not been well described. In addition, the cyclostomes have no distinct exocrine pancreatic structure, while the intestinal epithelium produces a peritrophic membrane, inside of which digestion takes place by interaction of extracellular enzymes (Nilsson & Fänge, 1970). So far, the teleost pancreas has been considered as "scanty" pancreas. Therefore, it is important to reveal the detailed morphology of teleost pancreas to obtain insight into evolution of the pancreas in vertebrates. Furthermore, in addition to evolution of the pancreas, zebrafish is a useful model for the study of tissue regeneration. They have highly regenerative abilities of fins, retina, spinal cord, heart, liver and kidney and other tissues (Gemberling *et al.*, 2013). In addition, they can regenerate lost β cells even at the adult stage (Moss *et al.*, 2009). However, the mechanism of pancreatic regeneration in fish still remains largely unknown.

In my doctoral thesis, I focused on medaka to obtain insights into the evolution and regenerative abilities of the vertebrate pancreas. This doctoral thesis consists of two chapters. In the first chapter, I investigated normal development and the entire structure of pancreas by establishing transgenic lines, which enabled me to simultaneously trace the development of endocrine and exocrine cells from the embryo to adult. In the second chapter, I examined the process of β cell regeneration at embryonic and adult stages using a transgenic line in which conditionally targeted β cell ablation was applied.

Chapter 1

Normal development of the pancreas in medaka

Introduction

The development of the pancreas in teleosts has been studied mainly in zebrafish. The combination of genetic, molecular and imaging analyses has made zebrafish an attractive model for the study of pancreatic organogenesis (Tiso *et al.*, 2009, Tehrani & Lin, 2011). In particular, transgenic lines generated using the promoters of the crucial genes, such as *insulin*, *pdx1* (Huang *et al.*, 2001), *somatostatin* (Li *et al.*, 2009) and *elastaseA* (Wan *et al.*, 2006), provide powerful platforms for live imaging of normal development as well as high-throughput drug screening (Kim *et al.*, 2006). It is now widely accepted that early development of the zebrafish pancreas proceeds in a manner similar to other vertebrates. Not only in early development, the zebrafish adult pancreas also shares many similarities in endocrine composition with the mammalian pancreas (Li *et al.*, 2009). However, zebrafish pancreas exhibits some unique features in organ architectures and organogenesis. For examples, zebrafish pancreas has one major big islet (principal islet) and a few later developing islets (secondary islets), instead of numerous small islets which are simultaneously developed and distributed in the entire pancreas in mammals (Field *et al.*, 2003, Li *et al.*, 2009). Zebrafish pancreas also develops as two buds that emerge from the intestine, but unlike mammals, the two buds are not equal in differentiation potency and contribution; the dorsal buds only give rise to endocrine cells forming the principal islet, while the ventral ones give rise to exocrine and duct cells and later on, to some extent, a small number of endocrine cells as secondary islets (Field *et al.*, 2003). The duct morphogenesis undergoes formation of

numerous small lumens within developing zebrafish pancreas, which subsequently to fuse to form a single tubular network, rather than branching morphogenesis of the pancreatic epithelium for mammals (Yee *et al.*, 2005).

For a better understanding of the development of digestive accessory glands in teleost fish, I have undertaken a thorough characterization of pancreatic development in medaka fish. The medaka has become a model vertebrate in developmental biology complementary to zebrafish (Takeda & Shimada, 2010), with the high quality draft genome (Kasahara *et al.*, 2007) and various developmental and spontaneous mutants (Ishikawa, 2000, Loosli *et al.*, 2000, Furutani-Seiki *et al.*, 2004, Kimura *et al.*, 2004, Kelsh *et al.*, 2004). There is a considerable evolutionary distance between medaka and zebrafish (110-160 myr apart), which is reflected in different gene repertories used for development and growth (Ishikawa, 2000, Loosli *et al.*, 2000). Thus the comparison of these two fishes would provide a comprehensive view of teleost pancreatic development. Development of medaka pancreas was previously studied, which only focused on the expression of a few marker genes during embryonic development (Assouline *et al.*, 2002). Our knowledge of medaka pancreas is thus still very limited especially the whole structure of adult pancreas.

In this chapter, to facilitate the study of medaka pancreas during both embryonic and adult stages, I have made two transgenic lines in which the expression of *pdx1* and *ptf1a* is visualized in different colors. I have characterized endocrine and exocrine differentiation and morphogenesis in medaka pancreas by a combination of live imaging of these transgenic lines, *in situ* hybridization and immunohistochemistry

using currently available molecular markers from embryo to adult. This analysis revealed some unique characteristics of adult pancreas in teleost.

Results

Generation and characterization of two stable transgenic medaka lines, *pdx1-EGFP* and *ptf1a-mCherry*

Pdx1 and Ptf1a are essential transcription factors co-expressed in pancreatic progenitors (Burlison *et al.*, 2008). These factors are known to contribute to induction and differentiation of the pancreas in vertebrates. I chose these two genes because they are expressed simultaneously and distinctively in progenitors and their descendant, endocrine and exocrine cells. To trace expressions of these two genes in wild-type medaka, I established two transgenic lines (*pdx1-EGFP* and *ptf1a-mCherry*) by BAC-mediated transgenesis (Moriyama *et al.*, 2012). Wild-type BAC clones (ola1-164F11 and ola1-121I17) containing the *pdx1* and *ptf1a* genes were subjected to modifications in which each coding region was replaced with EGFP and mCherry, respectively (Fig. 3A, B). The injection of these BAC clones was done at the one-cell stage and the transgenic lines were established (*pdx1-EGFP*, 2 lines and *ptf1a-mCherry*, 3 lines). All transgenic fish largely recapitulated the endogenous expression pattern of the two genes like zebrafish (Huang *et al.*, 2001, Hesselson *et al.*, 2011), although detectable timing and region tended to be little earlier and wider (Fig. 4A-H), probably due to the difference in turnover rate of mRNA or protein. I crossed those lines to generate a double transgenic medaka (double Tg) in which both *pdx1* and *ptf1a* expression is simultaneously visualized in green and red, respectively.

ptf1a is broadly activated from stage 19 (2-somite stage), in the gut endoderm encompassing the region from which the pancreatic bud will emerge. Then, *pdx1*

expression becomes detectable within the expression domain of *ptf1a* expression with high in the anterior of the gut tube at stage 21 (6-somite stage) (Fig. 5A-D). This is the first stage that *pdx1* and *ptf1a* are co-expressed in the gut endoderm. At the pancreatic budding stage (stage 26-27; 22-somite stage), the dorsal bud develops in the anterior domain co-expressing the two genes ('db' in Fig. 5E-H). At this stage, the gut tube rotates clock-wise so that the original dorsal side faces towards right (Fig. 5E-H). At the same time, on the other side of dorsal budding, a bigger ventral bud emerges in the *pdx1*- and *ptf1a*-double positive endoderm ('vb' in Fig. 5E-H). By the onset of budding, *pdx1* expression has become stronger and more restricted into the dorsal bud (Fig. 5H).

Since Pdx1 is known to be required for endocrine cell differentiation, the strong expression of *pdx1* in the dorsal bud suggests that the two buds are distinct in differentiation potency even at the beginning of their budding. Supporting this idea, *ptf1a* expression is specifically elevated in the ventral bud at stage 28 (Fig. 6A, white arrow). As development proceeds, the strong *ptf1a* expression expands along the gut tube (Fig. 6B-G). At stage 35 (visceral blood vessel forming stage), the dorsal and ventral buds have already fused under the gut tube and form pancreatic anlagen with a *ptf1a*-negative single islet (Fig. 6F, white arrow). At stage 39 (hatching stage), the dorsal and ventral buds subsequently expand as a unified organ (Fig. 6D, G).

ptf1a was reported to be expressed in the dorsal part of the neural tube and retina, more precisely in neural progenitors of the retina, cerebellum, midbrain-hindbrain boundary, hindbrain and spinal cord (Hoshino *et al.*, 2005, Zecchin *et al.*, 2004). As expected, these tissues and cells expressed mCherry in the

ptf1a-mCherry Tg line (data not shown).

Expression of endocrine cell differentiation marker genes

To verify the above fluorescent expression and relate it with normal medaka pancreatic cell differentiation, I have conducted thorough expression analysis using specific pancreatic markers by whole-mount *in situ* hybridization and immunohistochemistry. I first focused on markers for endocrine cells, *pdx1*, *nkx6.1*, *nkx6.2* and *nkx2.2*. *In situ* hybridization first detected the *pdx1* gene activity in the anterior gut tube at stage 21 (Fig. 7A); *pdx1* expression is relatively broad in the gut tube, expanding posteriorly, and at stage 26, the dorsal and ventral buds emerge from the gut tube in this *pdx1*-positive region (Fig. 7B-F). This temporal and spatial pattern of *pdx1* transcription is largely consistent with that observed in the *pdx1-EGFP* Tg line. Although little apparent difference in intensity between ventral and dorsal bud in Figure 7F, histological sections of stained samples confirmed that endogenous *pdx1* expression in the dorsal bud is stronger than that of ventral one (Fig. 7Y). Thus, I concluded that the strong GFP signal in *pdx1-EGFP* Tg dorsal bud reflects the elevated levels of endogenous *pdx1* expression.

The homeobox genes *nkx6.1* and *nkx6.2* are involved in differentiation of α- and β-cells in mice (Sander *et al.*, 2000). In zebrafish, both *nkx6.1* and *nkx6.2* are expressed in a row of endodermal cells located immediately above the yolk syncytial layer and neural tube at the 4-somite stage onward (Binot *et al.*, 2010). In medaka, *nkx6.2* expression is first detectable at stage 21 in a region similar to zebrafish (Fig. 7M),

and it becomes restricted to the presumptive pancreatic region from stage 23 (Fig. 7O-R). Medaka *nkx6.1* is strongly expressed in the posterior neural tube at earlier stages, but is also activated in the pancreatic region at stage 23 (Fig. 7I). However, as compared with *nkx6.2*, the expression levels are very weak (Fig. 7I-L). *nkx2.2*, known as a gene essential for maturation of β-cells in murine islets (Sussel *et al.*, 1998), is expressed in the medaka gut endoderm at around the same timing of *pdx1* activation (Fig. 7S). Notably, the pattern of *nkx2.2* expression is similar to that of *nkx6.2* (Fig. 7S-X).

I then examined the expression timing of differentiation markers for endocrine cells by whole-mount *in situ* hybridization and immunohistochemistry. Islet1 is expressed in all endocrine cells and required for the maturation of endocrine pancreas (Karlsson *et al.*, 1990, Du *et al.*, 2009). Islet1 protein is detected from stage 23 (Fig. 8C-F) onward in the *pdx1*-expressing region, especially higher in the prospective dorsal bud region. It was reported that the dorsal pancreatic bud exclusively gives rise to endocrine cells in zebrafish (Field *et al.*, 2003). The same could be true for medaka; Islet1 protein is detected only in the dorsal bud at the budding stage and importantly nearly all cells are positive for the anti-Islet1 antibody (Fig. 8U). It suggests that strong *pdx1* expression cause endocrine cell differentiation in the dorsal bud (Fig. 5H, 7Y).

Insulin is produced by β cells and its expression is nearly identical to that of Islet1 (Fig. 8I-L). Somatostatin, produced by δ cells, become detectable little later from stage 25, a stage just prior to the budding stage (Fig. 8Q-R). Glucagon production in α cells is even later and detected at stage 29, after the budding stage (Fig. 8T). Thus, the differentiation timing is different among three major endocrine cells (α, β and δ cells)

constituting the medaka principal islet. This order of expression is largely consistent with that observed in zebrafish pancreas: *insulin* is the first hormone gene to be activated at the 16-somite stage and *somatostatin* and *glucagon* are activated later at the 20-somite stage and 24 hpf (hours post fertilization), respectively (Argenton *et al.*, 1999). However, *glucagon* and *somatostatin* in zebrafish are initially expressed in extra pancreatic regions (eg. *somatostatin* in the floor plate and *glucagon* in posterior endoderm region), while those ectopic expressions in zebrafish were never observed in medaka but confined to the *pdx1*-positive region.

Exocrine cell differentiation starts after the budding stage

I also investigated the expression of exocrine markers by whole-mount *in situ* hybridization. *In situ* hybridization first detected *ptf1a* expression at stage 28 in the ventral bud (arrowhead in Fig. 9B). This stage corresponds to the stage when the elevated expression of *ptf1a* is observed in the *ptf1a-mCherry* Tg fish (Fig. 6A). Ptf1a is known to participate not only in exocrine differentiation but also in early pancreatic specification (Krapp *et al.*, 1998, Kawaguchi *et al.*, 2002). In addition, these different functions are regulated by graded levels of Ptf1a (Dong *et al.*, 2008). My result appears to reflect this notion; the *ptf1a-mCherry* Tg medaka exhibits weak but significant signals, which would represent its early function in progenitor cells, while at later stages, *ptf1a* expression is detected the region derived from ventral bud (arrowheads in Fig. 9C, D).

Ela3l, trypsin and amylase are produced by pancreatic exocrine cells and

secreted into ducts as pancreatic juice. Transcription of these genes occurs simultaneously in the *ptf1a*-positive region at stage 33 (arrowheads in Fig. 9F, H, J).

From my results of expression timing, it is suggested that medaka pancreas undergoes induction, endocrine cell differentiation, exocrine cell differentiation phases as summarized in Fig. 10.

Morphology of pancreas in adult medaka

Thus far, little is known about the gross morphology and structure of adult pancreas in fish, especially the exocrine component. By making use of my double Tg fish, I described the morphology and structure of adult pancreas in medaka. When the fat tissue, which fills the body cavity, was removed on the right side of the medaka trunk, the gallbladder and liver were visible (Fig. 11A). After removal of the gallbladder and liver, I observed that mCherry- (*ptf1a*-) positive cells were scattered in the mesentery, making ductal connections with the gut tube (Fig. 11B, C). These ducts form a net-like structure within the mesentery (Fig. 12A). Histological analysis demonstrated that cells positive for mCherry and Amylase (acinar cells marker) contribute to the ductal structure in the mesentery, together with unlabeled cells (putative duct cells) (Fig. 12B-D). Unlike mammalian pancreas that usually develops a single connection (Slack, 1995), the medaka exocrine pancreas establishes numerous direct connections with the gut tube (Fig. 13).

Aggregates of EGFP- (*pdx1*-) positive cells are located in the anterior region of the ductal network (Fig.11C). It is known in zebrafish that there are two types of

Langerhans islets named principal islet and secondary islet; the principal islet is generated directly from the dorsal bud, while small secondary islets are scattered along the gut tube (Tiso *et al.*, 2009). The origin of secondary ones is yet to be determined. In medaka, I have also observed two types of islet, a principal islet (arrows in Fig. 14A, B) and secondary islets in adult medaka (arrowheads in Fig. 14A, B). Secondary islets are much smaller in size; the size of principal islet is about 400-900 μm in diameter, whereas about 70-500 μm for secondary islet. Both islets contain major endocrine cells and thus they both are functional units, as indicated by combined immunostaining (Insulin and Somatostatin) and *in situ* hybridization (*glucagon*) (Fig. 15A-J).

Secondary islets are emerged at different timing from principal islet

I examined the timing of secondary islet development, using the *pdx1-EGFP* Tg fish. Near the principal islet, a group of cells weakly expressing EGFP appeared in the fat tissue after 20 days post-fertilization (dpf) (arrowhead in Fig. 16A). At 1.5 months post-fertilization (mpf), this cell aggregate becomes more evident as the levels of EGFP expression increase (arrowhead in Fig. 16B). At 2.5 mpf, the number of secondary islets increased to 2 or 3 (arrowheads in Fig. 16C). The precise timing of secondary islet development was hard to be determined by using *pdx1-EGFP* Tg fish, because *pdx1* expression was not confined to β cells completely during juvenile. Indeed bile ducts, adjacent to secondary islets, also weakly positive for *pdx1-EGFP* throughout development (Fig. 14A, B). Thus, I examined the *insulin* transgenic fish made for the study of β cell regeneration in which EGFP fused with Nitroreductase (NTR) is

expressed under the insulin promoter (detail explanation in the next Chapter). I found that insulin positive cells outside the principal islet first appeared around 16 dpf (white arrow in Fig. 16D). Adult fishes finally have 2-5 secondary islets. Principal islet and secondary islets are gradually increasing their size as body size growing (Fig. 17). In addition, female fishes tend to have more number of secondary islets than male (Fig. 18).

Discussion

In the present study, I have generated stable transgenic lines using BAC recombination technique in which EGFP and mCherry expression recapitulate endogenous *pdx1* and *ptf1a* expression, respectively. These transcription factors are known to be essential for pancreas induction and later differentiation of endocrine and exocrine cells (Burlison *et al.*, 2008, Kawaguchi *et al.*, 2002). The double Tg line enabled me to simultaneously visualize endocrine and exocrine cells in developing pancreas from embryo to adult. Thus far, transgenic zebrafish lines have been made using *pdx1*, *ptf1a*, *insulin*, *elastaseA,* and *somatostatin* promoters (Huang *et al.*, 2001, Wan *et al.*, 2006, Li *et al.*, 2009, Godinho *et al.*, 2005). In my doctoral study, combined with expression analyses of various marker genes, I have demonstrated conserved and specific features of development and structure of pancreas in fish.

Morphogenesis of medaka pancreas during early development

pdx1- and *ptf1a*-co-expressing cells were first identified in the anterior of the gut endoderm at stage 21 (Fig. 5A, C, D). They could be the most earliest detectable pancreatic progenitor cells in medaka embryos. At stage 27, dorsal and ventral buds are simultaneously emerged on both sides of the gut endoderm (Fig. 5E, G, H). The timing of budding in medaka contrasts with that in zebrafish because the two buds appear in different timing in zebrafish, 24 hpf for the dorsal and 40 hpf for ventral bud (Field *et al.*, 2003). At the budding stage, *pdx1* expression in the dorsal bud becomes stronger

than that in ventral bud (Fig. 5E, H), suggesting that differential properties between the two buds are already established at the initial phase of bud development. Indeed, like zebrafish, the dorsal bud in medaka preferentially gives rise to endocrine cells since the expression of *insulin*, Somatostatin and *glucagon* is confined to the dorsal bud region. In mammals, by contrast, no such preference has been observed; they appear to have equal differentiation potency (Jensen, 2004). In spite of this, the mechanisms of bud induction could be different between the two buds in mammals. The dorsal pancreatic bud develops in close association with the notochord, while the ventral one develops under the influence of developing liver and bile duct epithelium (Jensen, 2004).

ptf1a expression becomes elevated after the budding stage in medaka, and such strong expression extends over the gut tube (Fig. 6). In mouse embryos, the low levels of Ptf1a promote the endocrine fate, whereas high levels repress the endocrine fate but instead promote the exocrine fate (Dong *et al.*, 2008). Consistent with this previous study, the change of *ptf1a* expression levels in medaka appears to mark the turning point from the pancreas induction to exocrine differentiation stages. In zebrafish, it was reported with the *elastaseA-gfp* transgenic line that exocrine pancreas broadly extends along the gut endoderm (Wan *et al.*, 2006). The similar expansion was observed in the *ptf1a-mCherry* Tg medaka. As the gut gradually forms loops at later stages, exocrine cells in this region proliferate to spread the pancreatic anlagen and invade into the mesentery.

Endocrine cells and exocrine cells in medaka pancreas

Differentiation markers of endocrine cells, *insulin*, Somatostatin, and *glucagon* are sequentially activated from stage 23. In zebrafish, *insulin* is the first hormone gene to be expressed, and both *somatostatin* and *glucagon* are initially expressed in an extra-pancreatic region at the 16-somite stage (Argenton *et al.*, 1999). In medaka, by contrast, cells expressing Somatostatin and *glucagon* are only seen in the dorsal bud that exclusively contributes to the principal islet.

Ptf1a is an important transcription factor for exocrine cell differentiation. In this study, *in situ* hybridization fails to detect the early stage of its weak expression. This is probably due to lower sensitivity of *in situ* hybridization. Alternatively, the promoter used in the present study did not faithfully recapitulate the endogenous activity. I think that the former is more likely because the early expression of *ptf1a* was detected by PCR and found to be essential for early pancreatic specification in the mouse (Krapp *et al.*, 1998, Kawaguchi *et al.*, 2002). Strong *ptf1a* expression was observed at stage 28 and onward, after the budding stage, which is essential for the endocrine program (Krapp *et al.*, 1998). Differentiation markers of exocrine cells, *ela3l*, *trypsin*, and *amylase*, start to be expressed at stage 32. This timing coincides with the onset of the expansion of exocrine cell populations along the intestine.

As summarized in Fig. 10, medaka pancreas undergoes the process of induction, endocrine cell differentiation, and exocrine cell differentiation phases during organ formation of pancreas. This ordered process is conserved among vertebrates (Jensen, 2004, Tiso *et al.*, 2009) and thus could be a basic way of pancreatic

development in vertebrates.

Adult exocrine pancreas in medaka

The whole structure of teleost adult pancreas was visualized for the first time in the present study, using the double Tg fish. In zebrafish, the exocrine pancreas is a dispersed organ comprised of a branching network of ducts between loops of intestine as microscopically shown by anti-cytokeratin antibodies (Yee *et al.*, 2005). In medaka, the exocrine network labeled by mCherry (*ptf1a*) fluorescence were shown to spread in the mesentery, and many ductal structures were found to be connected to the gut tube in the broad area from the anterior to the end of the intestine (Fig. 12A). Multiple connections with the gut tube is one of the unique features of medaka pancreas, since the mammalian exocrine system is connected to the intestine duodenum via papilla Vater, a single duct formed by the union of the pancreatic duct and the common bile duct (Slack, 1995). This feature could be related to the fact that medaka has no stomach in their digestive tract (Castro *et al.*, 2014). Such agastric fish may require multiple connections with exocrine pancreas so as to receive pancreatic juices (digestive enzymes) in much broader areas. As the functional subdivision of the gut tube proceeded during evolution, the morphology of pancreas would then have been changed accordingly. Of course, the conservation of this unique structure in teleosts awaits further studies in zebrafish and other fish groups.

Secondary islets in teleost fish

The adult endocrine mass in zebrafish and medaka is organized into a single large islet, the principal islet, which is derived from the dorsal pancreatic bud. In addition, there are several small clusters named secondary islets present anterior to the principal islet (Li *et al.*, 2009). These extra islets newly develop at 76 hpf in zebrafish (Field *et al.*, 2003). Similarly, in medaka, 2-5 secondary islets were observed in adult, but the first secondary islet emerges at 16 dpf, which was much later than zebrafish. At the present, the origin of secondary islet is not known, but in medaka, my observation suggests that they develop independently of the principal islet as no connection between the two cell populations was detected. In mammals, endocrine cells aggregate into clusters during migration in a pancreas anlagen throughout the neonatal period (Yesil & Lammert, 2008). Once islets are formed, islets are generated by self-duplication rather than stem cell differentiation (Dor *et al.*, 2004), though their proliferation rate is very slow compared to other cell types (Teta *et al.*, 2005). By contrast, the number of secondary islets gradually increases in medaka after hatching and both of principal and secondary islets increasing their size related to their body size (Fig. 17). Intriguingly, it was reported in zebrafish that the number of secondary islets might depend on intensity of feeding (Li *et al.*, 2009, Wan *et al.*, 2006). Furthermore, I demonstrate here that it is also sex-dependent (Fig. 18). All these facts imply that the number of secondary islets is regulated by physiological environment and the teleost islet has flexibility in its size and number, while the mammal islet is stable. This feature could account for the high ability of adult pancreas regeneration in fish as compared with mammals (Moss *et al.*, 2009).

Chapter 2

The process of β cell regeneration in medaka

Introduction

As described in the Chapter 1, medaka pancreas shares many characteristic features with mammals in terms of the cellular composition of islets and developmental processes. Thus, medaka could be a model to study diseases of the pancreas.

Zebrafish is known to have highly regenerative fins, retina, spinal cord, heart, liver and kidney and other tissues (Gemberling *et al.*, 2013). As for pancreas, zebrafish was shown to regenerate β cells at embryonic and adult stages after their loss (Curado *et al.*, 2007, Pisharath *et al.*, 2007, Moss *et al.*, 2009). However, these regenerative abilities were lost during vertebrate evolution. In mammals, for example, regeneration takes place in limited tissues, such as skeletal muscle, liver and blood. Actually, mammalian embryos heal wounds rapidly and perfectly, while wound healing in adult is imperfect and generally results in fibrosis and scar contracture due to poor regeneration of epidermal and dermal structures (Redd *et al.*, 2004). On the other hand, adult teleost fishes still retain the high ability of regenerating their lost body part (Gemberling *et al.*, 2013). In mammalian pancreas, β cells are known to have a long life span with a very slow turn-over rate (Teta *et al.*, 2005), and pancreas, when damaged, does not fulfill the damaged part properly, though its cell number increases to some degree. Thus, the mammalian pancreas has insufficient capacity to regenerate itself.

The question of how this difference in regeneration ability emerged during evolution has attracted many researchers including myself. Despite many previous works with model animals, the mechanisms underlying cell and tissue regeneration

remain largely elusive, and essentially nothing is known about genetic factors that determine the capacity of tissue regeneration. Recently, it was suggested that epigenetic remodeling occurs during regeneration (Katsuyama & Paro, 2011). Thus, to address the above question, I think that both genetic and epigenetic approaches should be applied and that various models with a variety of regeneration capacity should be examined and compared. In this context, medaka is an attractive model, because it has advantages in genome science. Medaka has a compact genome (800 Mb), being only one-third the size of the human genome and less than half the size of the zebrafish genome (Takeda & Shimada, 2010). The draft genome sequence of medaka has been routinely updated by continuous efforts of Takeda and Morishita laboratories at the University of Tokyo. Furthermore, the epigenetic code at single-base resolution is being analyzed in medaka embryos and adult tissues by ChIP-seq and whole-genome bisulphite sequencing (Nakamura *et al.*, 2014). As for tissue regeneration, the high capacity of fin regeneration was previously reported in medaka (Katogi *et al.*, 2004, Sekimizu *et al.*, 2007). However, the regenerative ability of internal organs has not been well addressed and tools for the regeneration studies are not fully available in medaka.

Here, to investigate the regenerative ability of β cells in medaka and compare the ability with that reported in zebrafish, I have generated stable transgenic line that can specifically ablate β cells at any timing of interest. I use an *Escherichia coli* Nitroreductase (NTR)/Metronidazole (Mtz) system. This system relies on the NTR-mediated conversion of nontoxic prodrug into a cytotoxic agent (Lindmark & Müller, 1976, Anlezark *et al.*, 1992, Edwards, 1993). NTR is an enzyme that

metabolizes antibiotic Mtz into a DNA crosslinking cytotoxic product, leading to cell death. This approach has been successfully used for cell ablation in zebrafish (β cells, cardiomyocytes, hepatocytes) and medaka (osteoblasts) (Curado *et al.*, 2007, Pisharath *et al.*, 2007, Willems *et al.*, 2012). In the present study, I established the Tg medaka line, which expresses NTR as a fusion protein with EGFP under the control of the insulin promoter, and showed effective β cell ablation by Mtz prodrug treatment, followed by regeneration. I report the regeneration process of β cells after ablation in embryos and adults, and discuss the availability of this system and the unique feature of β cell regeneration in medaka.

Results

Establishment of the *insulin- EGFP-NTR* transgenic medaka

To apply the NTR/Mtz system for temporally and spatially controlled cell-ablation in medaka, I generated stable Tg lines in which an EGFP-NTR fusion protein is specifically expressed in β cells using the insulin promoter. From the previous report of Tg zebrafish (Huang *et al.*, 2001), I presumed that 3 kb fragment of the medaka insulin promoter region would be sufficient to drive endogenous expression of insulin, and I amplified the DNA fragment from the d-rR medaka genome by PCR. I injected the DNA construct shown in Fig. 19A into fertilized eggs and obtained two stable lines. The generated Tg lines were found to stably express GFP specifically in the β cells (Fig. 19B). I performed immunofluorescent staining for GFP and Insulin on *insulin-EGFP-NTR* Tg embryos at stage 39. I confirmed that only the insulin expressing cells expressed GFP (Fig. 19C, D). The two Tg lines established were nearly identical in terms of specificity and intensity of GFP expression, and thus I used the one selected line in the following experiments (referred to as *insulin-EGFP-NTR* Tg).

Ablation of β cell by Mtz treatment

To test whether β cells are sensitive to the cytotoxin converted from Mtz prodrug, *insulin-EGFP-NTR* Tg embryos were exposed to 10 mM Mtz/0.1 % DMSO, while the control group was incubated with 0.1 % DMSO. As for the other control, Mtz prodrug treatment was conducted on d-rR embryos to show that ablation was directly caused by NTR-mediated Mtz conversion. I chose stage 34 because this is the stage when all types

of endocrine cells have differentiated but the size of the principal islet is still small, allowing quicker and simpler assessment of ablation and recovery (Fig. 10). Furthermore, at this stage, secondary islets are not formed yet so that the principal islet was only targeted for β cell ablation. After incubation of embryos with Mtz for 6 days (4-10 dpf), they were subject to fluorescence microscopy observation for the presence of β cells. Mtz-prodrug treatment frequently caused the yolk sac edema either in d-rR and Tg embryos (Fig. 20A-C). This NTR-independent phenotype was transient and disappeared during larval stages, and most treated embryos developed and grew normally from larval to adult stages. However, significant reduction of fluorescence was observed in Mtz-prodrug treated Tg fishes, but not in DMSO-treated control (Fig. 20D-F). About half of the embryos (n = 15/27) showed no detectable fluorescence under fluorescent microscopy and the others showed reduced signals (Fig. 20E, F).

To examine if the loss or reduced signals of fluorescence was caused by ablation of β cells, I conducted immunostaining with anti-Insulin antibody for β cells, anti-somatostatin antibody for δ cells and DAPI for nuclei and confirmed that significant β cells reduction occurred only in Mtz-prodrug treated Tg fishes (Fig.20 G-I).

To confirm β cell ablation, I performed RT-PCR to examine the expression level of pancreatic marker genes. As shown in Fig. 21, only *insulin* expression was downregulated in Mtz prodrug treated Tg fishes, while the expression level of *glucagon* for α cells and *amylase* for exocrine cells was unchanged after the treatment. Taken together, I concluded that targeted ablation of β cells worked in my experimental

system.

The number of β cells is recovered following ablation

To investigate the regenerative capacity of β cells, both Mtz-prodrug treated and DMSO-treated fishes at 10 dpf were washed several times in fresh Mtz/DMSO-free water and allowed to develop for the following periods; 3 dpa (days post ablation), 7 dpa, 14 dpa, 30 dpa, and 150 dpa (5 months) (Fig. 22A). At 3 dpa, a small number of GFP-positive cells were visible within the islet region (Fig. 22B, G). At 7 dpa, a secondary islet first emerged in the extra principal islet region (Fig. 22C, H, arrow). It seemed that β cell ablation had no effect on the formation of secondary islets in terms of timing and position. GFP fluorescence in the principal islet of treated embryos was recovered to normal levels within 14 days, as compared to control (Fig.22D, I).

Interestingly, secondary islets tended to develop faster and bigger in Mtz-prodrug treated Tg than they did in control (Fig. 22E, J). I observed that in a 150 dpa fish, the size of some secondary islets was comparable or even bigger than that of the principal islet (Fig. 22F, K). Immunostaining using antibodies against Insulin and Somatostatin revealed that the proportion of β cells was maintained in enlarged secondary islets, suggesting that the component of endocrine cells did not change (Fig. 23).

β cell ablation in adult medaka

I then investigated whether β-cell regeneration in medaka takes place even at the adult

stage. The adult stage is particularly interesting because I can ablate both β cells in the principal and secondary islets.

I injected 1 mg/g Mtz into the peritoneal cavity everyday for 3 days, a single injection per day. One day after the last injection, I observed the significant loss of fluorescence in the islets regions (Fig. 24A, B). Sections stained with anti-Insulin antibody showed that positive signals (Cyan) for Insulin were detected in Mtz-injected fish, but they did not co-localize with DAPI (Blue) (Fig. 24C, D). Thus I concluded that they are dying β cells and nearly all β cells are ablated by peritoneal Mtz injection. The treatment also disrupted the structure of the islet (Fig. 24C, D). Injected fishes were then assessed for recovery at one week and 2 weeks after the last injection (Fig.25A). Contrary to my expectations, GFP fluorescence did not recover within 2 weeks, although a small number of GFP signals were observed (Fig. 25B, C).

Discussion

I generated the stable transgenic line, which enabled me to specifically ablate the β cell population in medaka at any timing from embryo to adult. Using this system, I have demonstrated that medaka has the high capacity of β-cell regeneration at least at embryo to larval stages.

The efficiency of targeted cell ablation by Mtz prodrug treatment

In the present study, I applied the NTR/Mtz cell ablation system to medaka. In the past, this system was successfully applied to tissue-specific cell ablation in zebrafish (Curado *et al.*, 2007, Pisharath *et al.*, 2007, Moss *et al.*, 2009) and medaka (Willems *et al.*, 2012). In previous reports using zebrafish embryos, substantial cell ablation was detected after 24-hour exposure to 10 mM Mtz. In medaka, on the other hand, efficient ablation was reported to require much stronger conditions such as 10 mM Mtz for at least 6 days for osteoblasts in developing embryos (Willems *et al.*, 2012). In the same way, for β cell ablation in adult zebrafish was achieved by a single intraperitoneal injection of 0.25 mg/g Mtz (Moss *et al.*, 2009), whereas in my study, diary injection of 1 mg/g Mtz for 3 days was required. I confirmed that a single injection only caused insufficient cell ablation in medaka adults (data not shown). The reason for different conditions required in medaka and zebrafish studies are not clear at the moment, but might be due to species difference because all zebrafish studies reported so far adopted less severe treatment for various cell lineages (Curado *et al.*, 2007). It is likely that medaka cells are more

tolerant to cytotoxins or NTR is less efficient in medaka cells. Treatment condition may also depend on a promoter used and integration site in each Tg fish. In any case, my study, together with the previous medaka one (Willems *et al.*, 2012), suggests that treatment conditions are highly variable depending on organisms used even when the similar strategy is used, and that higher dose and longer exposure of Mtz are generally required for ablation cells of interest in medaka as compared with zebrafish.

Furthermore, I noticed that Mtz prodrug has off-target toxicity on developing embryos, irrespective of the presence of NTR, because I observed the yolk sac edema in both wild-type and Tg embryos (Fig. 20A, C). This phenotype might be caused by dysfunction of kidney (Incardona *et al.*, 2004). Such toxicity was also reported in zebrafish by prolonged Mtz exposure (Curado *et al.*, 2007). However, this may not complicate my interpretation of the results, because the edema was transient and disappeared soon after hatching. Most treated embryos anyhow reached the adult stage with no apparent phenotype.

Regeneration of β cells in medaka

I succeeded in ablating nearly all β cells by Mtz prodrug treatment in medaka embryos (Fig. 20, 21), and described their recovering processes. After washing out Mtz, I observed a steady increase in fluorescence in the islet region. By 2 weeks after the treatment, treated Tg medaka larva showed enough recovery of fluorescence, which was almost comparable to that in control (Fig. 22). Rapid recovery of β cell population implies the existence of mechanisms with which to sense and maintain the size of β cell

mass.

The important finding of this study is that Mtz-treated Tg embryos/larva have larger secondary islets than controls, although they regenerated their principal islets property. This is the first to reveal a dynamic nature in development of secondary islets during regeneration processes. Indeed, previous studies with zebrafish did not focus on secondary islets in embryo-to-larval or adult stage regeneration of β cells, and thus, knowledge on the secondary islet in light of tissue regeneration had been very limited before my study. The secondary islet is a unique tissue which is only found in teleosts (Li *et al.*, 2009). The function of the secondary islet could be comparable to the principal one as described in Chapter 1; it has the cell-type component similar to that of the principal islet. However, they are formed at different developmental timing (16 dpf and later) and in different places. Under my experimental conditions (Mtz treatment from 4 to 10 dpf), secondary islets start to develop at least 4 days after ablation of β cells in the principal islet. Thus, lower levels of insulin or reduced number of β cells could affect the development of secondary islets. The physiological function of the secondary islet is still unknown, but my result suggests that it serves as a reservoir of endocrine cells and plays a regulative role in response to a change in the physiological environment. This leads me to speculate that endocrine cells in the secondary islet remain highly regenerative. It would be important to analyze this character of the secondary islet to understand a mystery of β cell regeneration.

In adult mammals, injured pancreas fails to undergo a significant replacement of lost tissue. In sharp contrast, adult zebrafish has the high capacity of β cell

regeneration; the recovery was reported to complete within 2 weeks (Moss *et al.*, 2009). Thus, I expected the similar regeneration ability in medaka adults, but this was not the case in my study. This suggests that the regeneration ability in pancreas becomes restricted as medaka grows but it does not in zebrafish. Generally speaking, during embryogenesis and larval development, tissue regeneration can be achieved through the continuous and prolonged developmental program, but this may not hold true for regeneration at the adult stage (Kawakami *et al.*, 2004). This could partly account for the observed species difference. However, I think, it would be premature to conclude that adult medaka has the limited ability of β cell regeneration. Definitely, I need to test various possibilities and conditions before I draw a conclusion. First, madaka may take much time to regenerate their β cell mass than zebrafish. Second, as mentioned above, the ablation condition used here was more severe than zebrafish, which may affect the regeneration process in the adult medaka pancreas. Indeed, the structure of islets were disrupted in injured adult fishes, suggesting that the conditioned used here could be too severe. These possibilities should be evaluated under various experimental conditions.

Finally, I have established the medaka system for targeted ablation of β cells, which provide a promising genetic tool to analyze the process and mechanism of regeneration of β cells.

General discussion

In my doctoral study, I established stable transgenic lines for the analysis of normal pancreatic development and regeneration of β cells in medaka. This study not only revealed the conserved development of pancreas in vertebrates but also unique structural features of the pancreas in teleosts. Furthermore, I found that medaka has a high capacity to regenerate β cells in immediate response to their loss during embryonic and larval stages.

Evolution of the pancreas in vertebrates

The pancreas is structurally conserved from amphibians to mammals, which is a compact organ containing the exocrine and endocrine components as demonstrated by a number of anatomical and histological studies (Slack, 1995). The development of the pancreas in those animals is also well conserved; two buds (dorsal and ventral) emerge from the anterior part of the intestine and later fuse to form a single anlagen (Pearl *et al.*, 2009, Ahnfelt-Rønne *et al.*, 2007, Jørgensen *et al.*, 2007). It is also known that the pancreas of cartilaginous fish consists of a compact organ. On the other hand, the teleost pancreas is known to be a diffused type except for a few species. A small number of islets are located mainly near the liver, but the exocrine tissue is dispersed broadly along the intestine. Despite this morphological difference, the present study, together with the previous zebrafish studies, demonstrated that teleosts develop their pancreas in the same way as other vertebrates. Actually, in dispersed pancreas, the endocrine cells are always

surrounded by the exocrine tissue as in a compact pancreas. However, I found one unique feature of the adult medaka pancreas that the exocrine tissue forms mesh-like structure and connects to the intestine at multiple points. Since this is the first description of the exocrine duct network in adult teleost fishes, I cannot say at the moment that this feature is conserved in the teleost lineage. However, if this is indeed conserved, I speculate that this structural difference could be related to the functional evolution of vertebrate intestine as discussed below.

Cyclostomes, earliest diverged vertebrates, have a short straight intestine with pancreatic exocrine and endocrine cells. Pancreatic exocrine cells are scattered in intestinal mucosa, and thus do not form a separate tissue or organ. Endocrine cells, consisting of only β and δ cells, differentiate independently of the exocrine tissue (Epple & Brinn, 1975). They are present as a single cell or a group (islet) and found in and around the bile duct without any connection to the exocrine tissue (Ostberg *et al.*, 1975, Ostberg *et al.*, 1976). Thus, I suppose that the teleost pancreas is an intermediate-type between this primitive pancreas and later evolved compact pancreas seen in many vertebrates.

My scenario of pancreas evolution is as follows (Fig. 26). At the beginning of vertebrate evolution, the primitive exocrine tissue and islets developed independently. Then the ability to produce the exocrine and endocrine tissue became restricted to a certain small region of the intestine, as the intestine underwent substantial morphological and functional differentiation such as elongation, turning and regionalization, and was finally confined to the anterior intestinal region in which buds

protrude from the intestinal wall, a ventral bud for exocrine and dorsal bud for endocrine cells. These two buds fuse into a single anlagen. Independently developed endocrine and exocrine tissues need to be integrated to react feeding stimuli as a single unit by vagal innervation. Further analysis of nerve distribution in teleost pancreas is needed to understand the mechanism of fusion of different two tissues. Teleosts have diffused type of pancreas, while the pancreas continued to change as vertebrates further evolved. The next important event is the formation of a compact organ, which took place first in amphibians, but a part of amphibians still have a diffused-type pancreas. In *Xenopus* embryos, the different differentiation potency between the two buds was reported to be maintained like teleosts. However, after fusion of the dorsal and ventral buds, the endocrine and exocrine (islet) components become intermingled and form a compact organ (Pearl *et al.*, 2009, Horb & Slack, 2002). The difference in differentiation potency between the two buds then became blurred in birds. In chicken embryos, the ventral bud gives rise to only exocrine cells, while the dorsal bud gives rise to mainly the endocrine, but also a small number of the exocrine cells (Matsuura *et al.*, 2009). Finally, the two buds became identical in differentiation potency in mammals, producing both exocrine and endocrine cells (Jensen, 2004, Jørgensen *et al.*, 2007).

Although I described the above scenario, essential questions remain largely unanswered, as to why this change in differentiation potency took place from amphibians to mammals and which genes in gene regulatory network were responsible for this change. Teleost models (medaka and zebrafish) with various important tools will be crucial in addressing these questions.

Characteristics of teleost-specific secondary islets

In the present study, I described a small group of endocrine cells called "secondary islet" localized outside the principal islet, which is derived from the dorsal bud. The secondary islet was first reported in zebrafish (Field *et al.*, 2003). Islets in other vertebrates are thought to have no subtypes, while in teleosts the size of secondary islets is smaller than that of the principal islet and they develop at different timing and in different places. Thus, the secondary islet is unique in teleost fishes, and is expected to have a distinct function albeit the similar component of endocrine cells.

My medaka and previous zebrafish studies have demonstrated that the secondary islet has at least two unique features in addition to the timing and place of development. First, the secondary islet changes it number under normal physiological condition. Indeed it increases even after early development and its number depends on sexes (Otsuka *et al.*, 2015). In zebrafish, feeding intensity is also known to affect the number of secondary islets (Li *et al.*, 2009, Wan *et al.*, 2006). This is in sharp contrast to mammals in which the number of islets is determined during early development and they maintain their number by self-duplication (Dor *et al.*, 2004). Second, the size and growth speed of secondary islets is increased in response to β cell ablation in the principal islet at the embryonic stage (Chapter 2). All these facts suggest that the teleost-specific secondary islet remains proliferative and functions in regulating the number of islets in response to a change in physiological conditions including injury to endocrine cells. Given this unique feature, further analysis focusing on the proliferation

of the secondary islet may help in understanding of β cell regeneration and pathogenesis of diabetes.

Conclusion

The basic aspect of pancreatic development, two buds from the intestine followed by their fusion into a single anlagen, is conserved within vertebrates, but I found some unique features in teleost pancreatic development such as distinct differentiation potency of the two buds and later developing secondary islets. Moreover, our analysis first reports the multiple connections between the exocrine network and gut in adult medaka, which could place the teleost pancreas halfway in the pancreas evolution from cyclostomes to mammals.

In addition, I established a conditional targeted cell ablation system in medaka to study the mechanisms of β cell regeneration. Using this system, I found that medaka embryos have the high capability of β cells regeneration and thus can be a good model for tissue regeneration. Furthermore, my observation of normal development and recovery processes of β cell ablation demonstrated that the teleost-specific secondary islets remain proliferative long after initial development completes, serving as a reservoir of endocrine cells prepared for normally changing and critical situations. Further studies of regeneration mechanism using my medaka model, in particular, focusing on the secondary islet, will be helpful in understanding of β cell regeneration.

Materials and methods

Fish strains

All studies of medaka (*Oryzias latipes*) were carried out using d-rR strain of a closed colony. Fish stocks were maintained under an extended photoperiod of 13.5: 10.5 h light: dark at 28°C. Under these conditions, medaka spawn daily within 1 hour of the onset of light for a number of consecutive days. Collected medaka embryos were sorted into medaka Hatching buffer, maintained at 28.5°C, and staged according to morphological criteria (Iwamatsu, 2004).

BAC modification by homologous recombination and transgenesis

Homologous recombination of the BAC clones was performed as previously described (Nakamura *et al.*, 2008). Generation of transgenic lines by BAC injection into embryos of the d-rR strain was performed as previously described (Nakamura *et al.*, 2008). I used the I-SceI meganuclease method to increase the frequency of successful germline transmission as previously described (Rembold *et al.*, 2006).

Generation of Tg

To clone the medaka *insulin* promoter region, a pair of PCR primers was designed based on medaka *insulin* genomic sequence in Ensembl. A 3-kbp fragment upstream of the start codon of the *insulin* gene was amplified by PCR. Nitroreductase (NTR), encoded by the *E.coli* gene *NfsB*, was isolated from *E. coli* genomic DNA by PCR.

These sequences were inserted into pEGFP vector (Clontech). I used the I-SceI meganuclease method as described above.

Whole-mount in situ hybridization

Embryos were fixed with 4% paraformaldehyde (PFA) in PBST (phosphate-buffered saline containing 0.1% Tween-20) overnight and dechorionated manually with forceps, then stored in MeOH at –20°C. After rehydration, embryos were permeabilized with proteinase K (10 μg/ml) at room temperature for 7-12 minutes (depends on developmental stages) and re-fixed with 4% PFA/PBST for 25 min. The specimens are washed five times in PBST. Hybridization was carried out at 65°C with digoxigenin-labeled probes overnight. Hybridized embryos were washed with 50% formamide/2xsaline-sodium citrate containing 0.1% Tween20 (SSCT), 2xSSCT and 0.2xSSCT, incubated in 0.2% blocking reagent (Roche) at room temperature for more than 2 hours, and then treated with anti-digoxigenin antibodies labeled with alkaline phosphatase (Roche) at 1:7000 dilution with 0.2% blocking reagent. The staining reaction was started by incubating medaka embryos with NBT/BCIP solution according to the protocol described for the NBT/BCIP ready-to-use tablets (Roche). The cDNAs used as the templates for the probes were described in Table 1.

Histology

Isolated tissues were fixed in 4% paraformaldehyde (PFA) in phosphate buffered saline (PBS) overnight, followed by dehydration with a graded series of ethanol (70%, 95%,

and 100%) and embedding in paraffin. Sections with 5 μm thicknesses were made using a microtome. Section fluorescent immunohistochemistry was performed using the following antibody: chick anti-GFP antibody (1:500, abcam), rabbit anti-Somatostatin antibody (1:500, abcam) and guinea pig anti-Insulin antibody (1:200, Dako). Specimens were incubated with blocking reagent (10% normal goat serum with 1% Triton X-100 in PBS), then incubated overnight at 4°C in primary antibody diluted with 10% normal goat serum with 1% Triton X-100 in PBS. The bound antibodies were detected by Alexa Fluor® 488 Goat anti-chicken IgG (H+L), Alexa Fluor® 555 Goat anti-rabbit IgG (H+L) and Alexa Fluor® 647 Goat anti-guinea pig IgG (H+L) diluted 1:500 with 1% Triton X-100 in PBS. For DAB staining, Living Colors® Full-Length GFP polyclonal antibody (1:500, Clontech) was used as a primary antibody and biotin-conjugated anti-rabbit IgG (1:250, Sigma) was used as a secondary antibody.

For whole mount immunostaining, samples were fixed in 4% PFA/PBS for 2 hrs at room temperature. Samples were permeabilized with 0.5% Triton X-100 in PBS at room temperature for 1.5 hrs, rinsed with PBS, and then incubated in 2% BSA, 10% DMSO, and 0.2% Triton X-100 in PBS at room temperature for 3 hrs. Mouse anti-Islet1 antibody (1:500, 39.4D5, DSHB), Living Colors® DsRed Polyclonal Antibody (1:200, Clontech), Rabbit anti-α-Amylase antibody (1:200, Sigma), and anti-cytokeratin 19 antibody (1:500, abcam) were used as a primary antibody. Biotin-conjugated anti-mouse IgG (Sigma) and biotin-conjugated anti-rabbit IgG (1:250, Sigma) were used as a secondary antibody at a 1:250 dilution. Samples were washed with PBSDT (1% DMSO and 0.1% Triton X-100 in PBS). Samples for HE staining, were embedded

in Technovit 7100 resin (Heraues-Kulzer) and sectioned with RM 2245 (Leica) at a 5-μm-thickness.

For combined immunohistochemistry and *in situ* hybridization, isolated tissues were fixed with 4% PFA/PBS for 6 hrs at 4°C, followed by dehydration in increasing gradients of ethanol (70%, 95%, and 100%) and embedding in paraffin. Sections with 5 μm thicknesses were made using a microtome. Specimens were incubated with 10% normal goat serum with 1% Triton X-100 in PBS, then incubated overnight at 4°C with primary antibody (guinea pig anti-Insulin antibody, 1:200, Dako; rabbit anti-Somatostatin antibody, 1:500, abcam) diluted with 10% normal goat serum in 1% Triton X-100/PBS. After post-fixation with 4% PFA/PBS, the sections were hybridized with the DIG-labeled *glucagon* probe (500 ng/ml) in a hybridization buffer at 58°C overnight. After rinsing, the sections were incubated with the blocking reagent (Roche) diluted with 0.1% Tween 20 in PBS. The sections were subsequently incubated with Alexa Fluor® 647 Goat anti-guinea pig IgG (H+L), Alexa Fluor® 488 Donkey anti-rabbit IgG (H+L) (diluted 1:500 for each) and alkaline phosphatase-conjugated anti-DIG antibody (diluted 1:1000, Roche) for 2 hrs. The alkaline phosphatase activity was detected using Fast Red Tablets (Roche) according to the manufacturer's instructions.

Mtz treatment

About Mtz treatment for embryos (stage 34), after dechorionation, the control group was kept in 0.1% DMSO in 1xYamamoto ringer. The other group was incubated in

10mM Mtz (Sigma) dissolved in 1xYamamoto ringer with 0.1% DMSO. Throughout the incubation period, embryos were kept in 4-well dishes at 28.5℃ in the dark. Media were replaced once a day.

About Mtz treatment for adult fish (10 month), Mtz was injected at 1.0 g/kg b.w. in Mtz was dissolved in 5 mmol/l citrate, pH 5, and then injected with 1 ml Syringe using 34G needle. The effectiveness of the injection was monitored by adding 0.25% phenol red.

RT-PCR

RT-PCR analysis was performed using total RNA of medaka embryos. Total RNA was isolated from DMSO or Mtz treated medaka embryos at 0 dpa using ISOGEN (Nippon gene), according to the manufacturer's instructions. First-strand cDNA was prepared from 1 μg total RNA using an oligo d(T) primer and SuperscriptIII reverse transcriptase 47 (Invitrogen) and cDNA fragments were obtained by PCR with the primers described in Table 2.

Figures

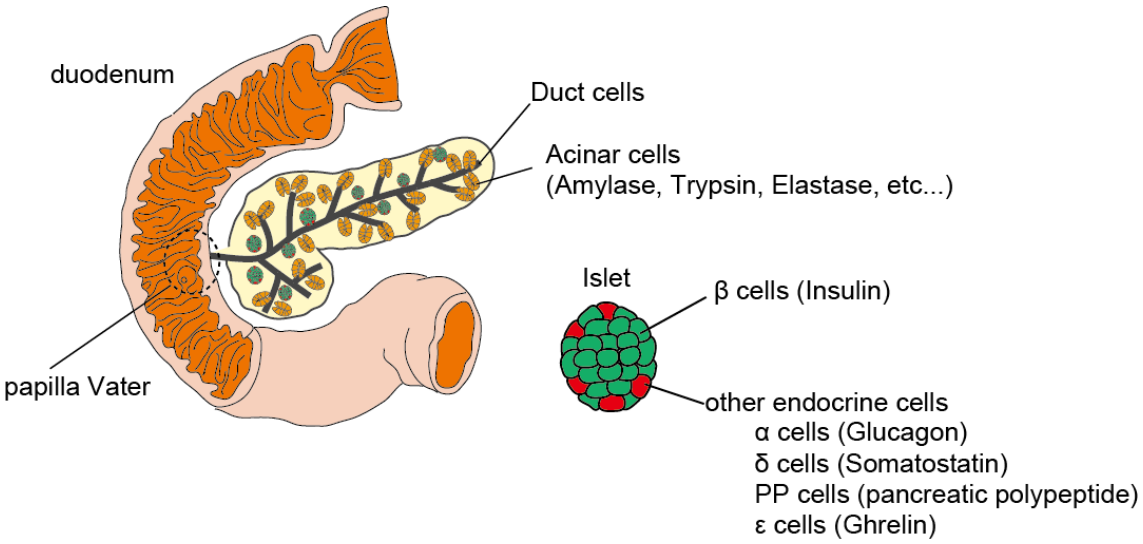

Fig. 1. Diagram of mammalian pancreas morphology

Schema of mammalian pancreas. The pancreas contains exocrine cells (Acinar cells and duct cells) and endocrine cells. Five types of endocrine cells form a cluster (islet). The duct of pancreas is connected to the duodenum via papilla Vater.

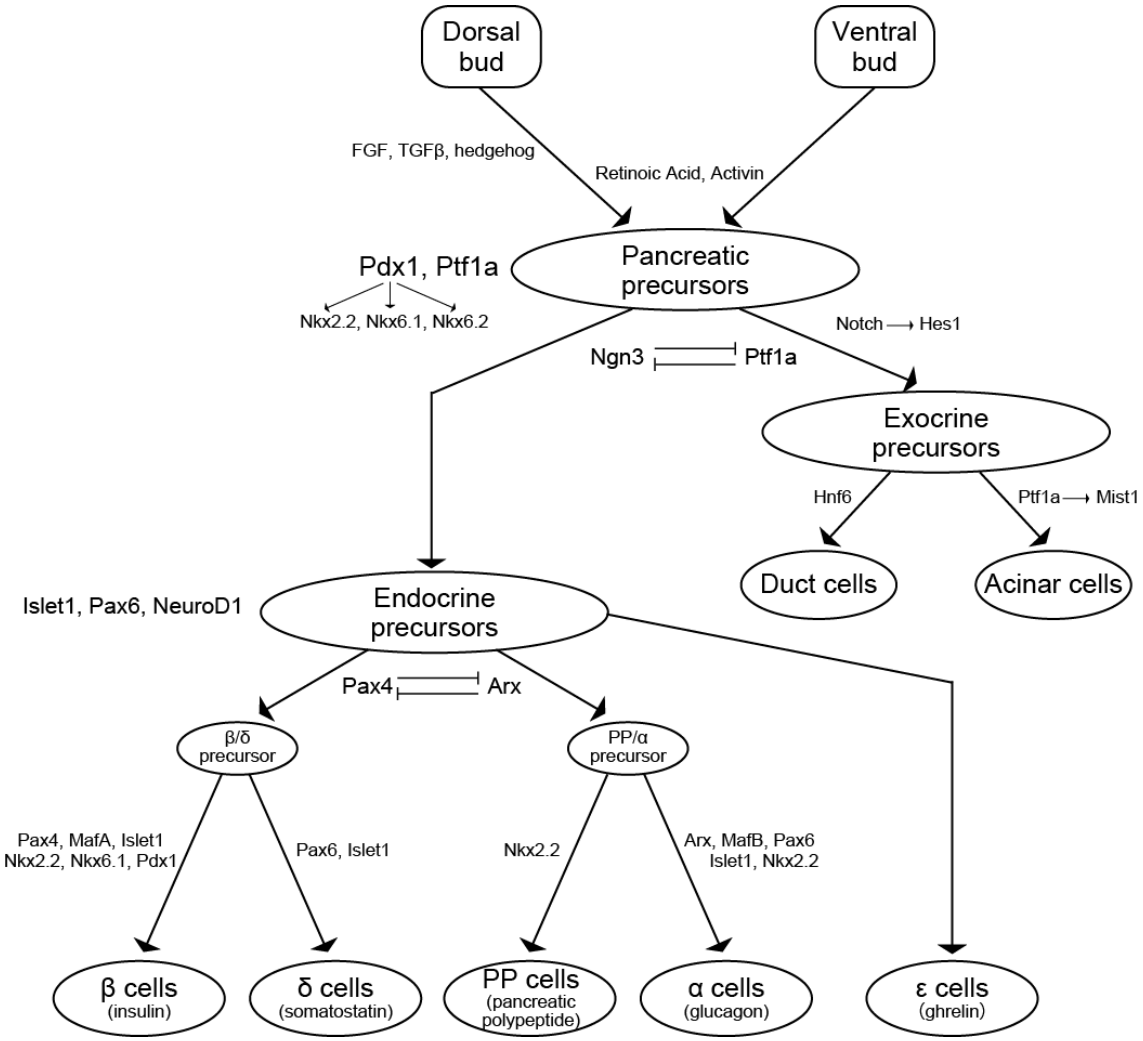

Fig. 2. Gene regulatory network during the development of the pancreas

Many transcription factors and signaling molecules are known to be involved in initial pancreatic development. Combination of some transcription factors and proper expression timing is essential for various types of pancreatic cell differentiation.

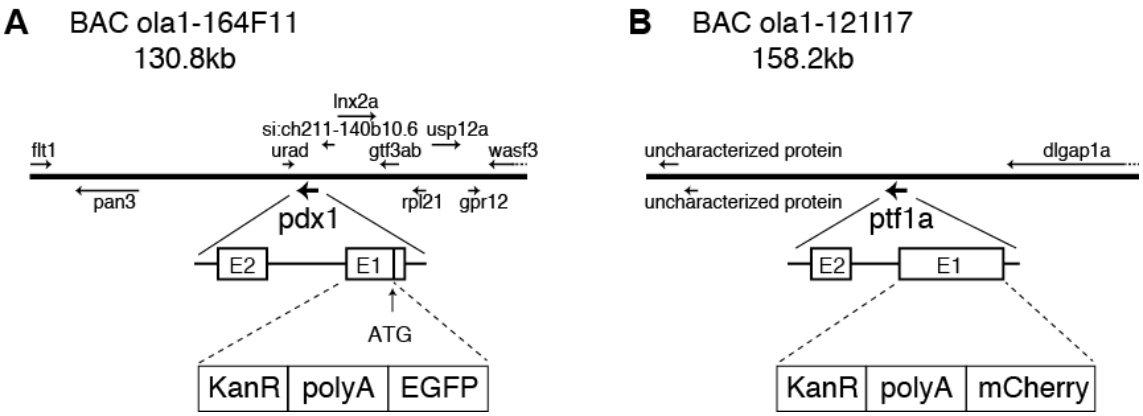

Fig. 3. Diagram of BAC constructs used for making Tg lines

(**A**) A diagram of BAC modification to replace the 1st exon of *pdx1* gene with enhanced green fluorescent protein (EGFP) at the start codon. (**B**) A diagram of BAC modification to replace the 1st exon of *ptf1a* gene with mCherry at the start codon.

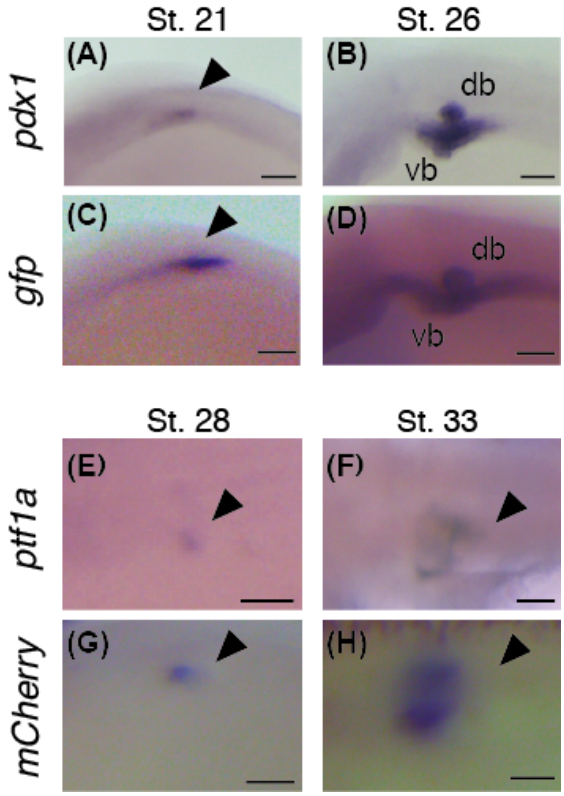

Fig. 4. Recapitulation of endogenous expression pattern of *pdx1* and *ptf1a* in the Tg line

(A, B) *pdx1* endogenous expression at stage 21 (A) and stage 26 (B) in wild-type embryos. **(C, D)** *gfp* mRNA expression at stage 21 (C) and stage 26 (D) in *pdx1-EGFP* transgenic medaka embryos, showing that *gfp* expression is nearly identical to endogenous *pdx1* expression. **(E, F)** *ptf1a* endogenous expression at stage 28 (E) and stage 33 (F). **(G, H)** *mCherry* mRNA expression at stage 28 (G) and stage 33 (H) in *ptf1a-mCherry* transgenic medaka, showing that *mCherry* expression is nearly identical to endogenous *ptf1a* expression. Lateral view and anterior to the left. Scale bars, 100 μm. db, dorsal bud; vb, ventral bud.

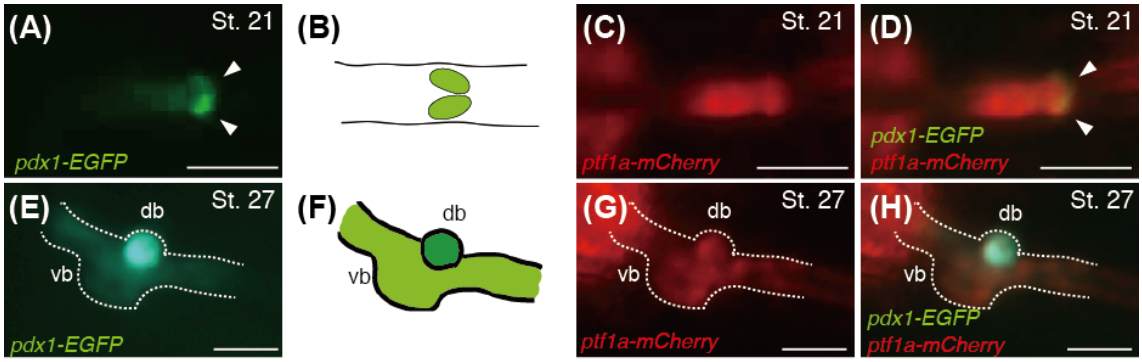

Fig. 5. Budding of pancreatic anlagens from the gut tube during early somite stages

(A, C, D) Dorsal view of the double Tg embryo at stage 21. Anterior trunk region viewing EGFP (A), mCherry (C), and combination of EGFP/mCherry (D). Co-expression of *pdx1* and *ptf1a* is first detected at stage 21 (white arrowhead). **(B)** A schema of panel A to show the position of the earliest *pdx1* expression of pancreas primodium (green). **(E, G, H)** Dorsal view of the double Tg embryo at stage 27. Anterior trunk region viewing EGFP (E), mCherry (G), and combination of EGFP/mCherry (H). White dotted lines show outline of the gut tube. Two pancreatic buds emerged from the gut tube. In the dorsal pancreatic bud (db), a strong EGFP expression can be detected. *pdx1* and *ptf1a* are still co-expressed in both of dorsal and ventral bud at stage 27. **(F)** A schema of panel E to show the strong *pdx1* expression of dorsal bud (dark green) compared to other region (light green). Anterior to the left in A-H. Scale bars, 100 μm. db, dorsal bud; vb, ventral bud.

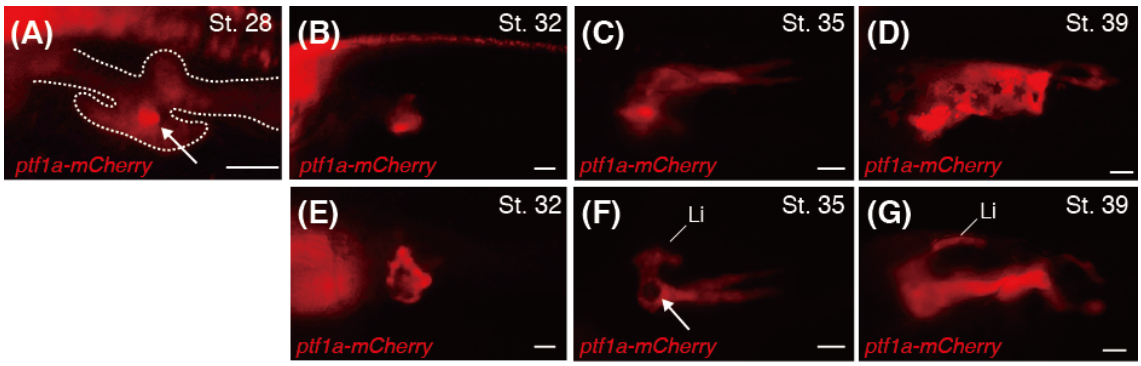

Fig. 6. Extension of the ventral bud along the gut tube after the segmentation stage

(A) Ventral view of the Tg embryo at stage 28. **(B, C, D)** Lateral view of the Tg embryo at stage 32 (B), stage 35 (C), and stage 39 (D). White dotted lines show outline of the gut tube. A strong ptf1a expression starts at stage 28 (a white arrow in A), and expands along the gut tube to posterior. **(E, F, G)** Ventral view of the Tg embryo at stage 32 (E), stage 35 (F) and stage 39 (G). The white arrow in F shows the ptf1a-negative principal islet. Ventral buds start to surround dorsal buds at stage 32. Dorsal and ventral buds are fused and form an early pancreatic organ at stage 35. Anterior to the left in A-G. Scale bars, 100 μm. li, liver.

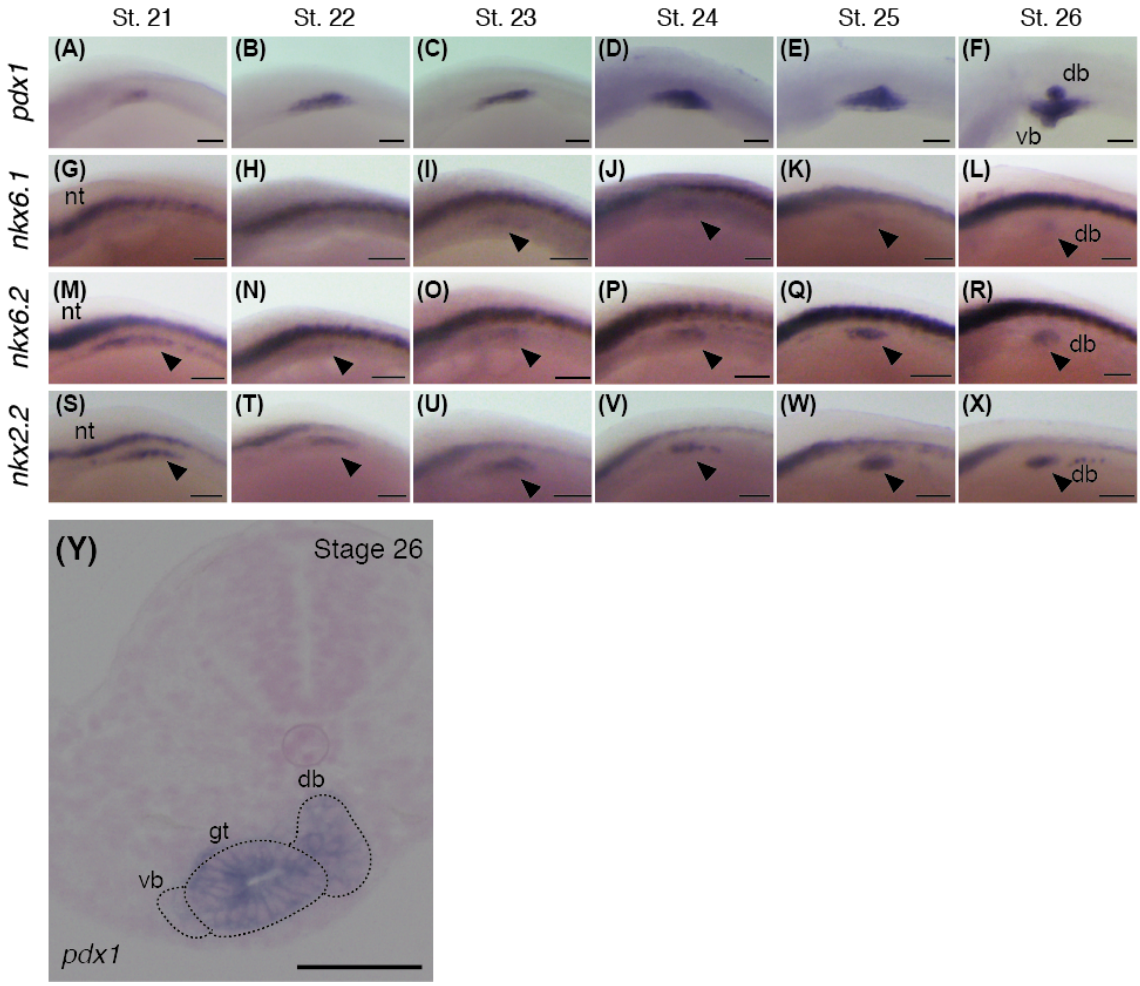

Fig. 7. Expression of transcription factors required for pancreas induction

(A-X) *in situ* hybridization for *pdx1* (A-F), *nkx6.1* (G-L), *nkx6.2* (M-R), *nkx2.2* (S-X) from stage 21 to stage 26. *pdx1* expression starts at stage 21 in the anterior gut tube region (A). Dorsal and ventral pancreatic buds emerge at stage 26 (F). *nkx6.1* is expressed in the neural tube (nt) at stage 21. From stage 23, very weak expression is detected in the pancreatic precursor region (black arrowheads). *nkx6.2* expression is detected at stage 21 in the neural tube and in

a row of cells located immediately above the large syncytial yolk cell layer. Expression is restricted into the pancreatic precursor region from stage 23 (O-R, black arrowheads). The expression pattern of *nkx2.2* is almost same as the *nkx6.2* expression (S-X, black arrowheads). **(Y)** Histological section of panel F. *pdx1* expression in the dorsal bud is stronger than that of ventral one. Lateral view and anterior to the left in A-X. Scale bars, 100 μm (A-X) and 50 μm (Y). db, dorsal bud; vb, ventral bud; nt, neural tube; gt, gut tube.

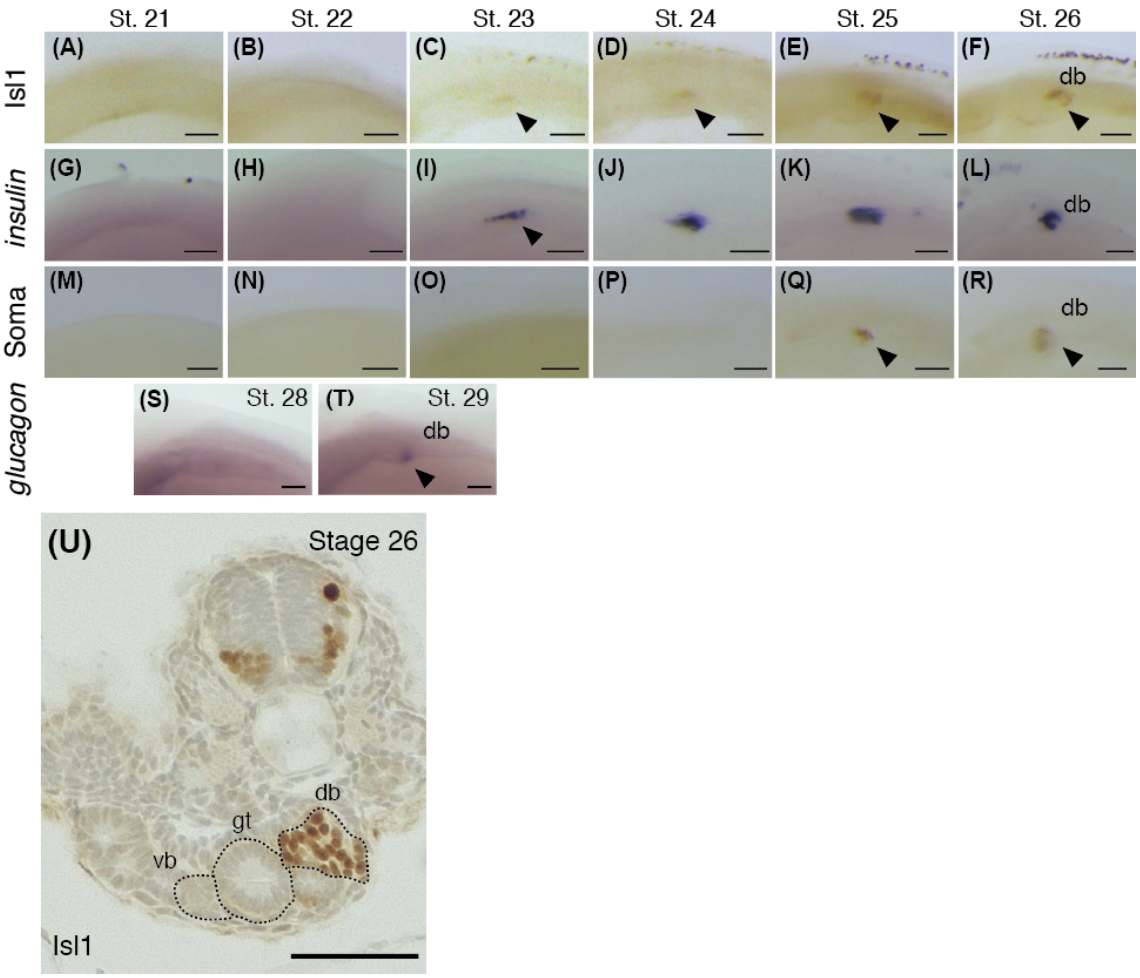

Fig. 8. Expression of endocrine cell markers

(A-F, M-R) Immunohistochemistry for Islet1 (A-F, Isl1), Somatostatin (M-R, Soma). **(G-L, S-T)** *in situ* hybridization *for insulin* (G-L), *glucagon* (S, T). Islet1 protein was detected from stage 23 in the gut tube (C-F, black arrowheads). From stage 23, endocrine cell differentiation starts. At stage 26, Islet1 protein is clearly visible in the dorsal bud. *insulin* expression starts from stage 23 (I, black arrowhead). β cell differentiation starts from stage 23. Somatostatin protein is

detected from stage 25 (Q, R, black arrowheads). δ cell differentiation starts slightly later than β cell differentiation. *glucagon* expression is detected from stage 29 (T, black arrowhead). α cell differentiation starts later than the other 2 endocrine cells. **(U)** Histological section of panel F. In the dorsal bud, all cells are Islet1-positive, whereas the ventral bud has no Islet1-positive cells. Lateral view and anterior to the left in A-T. Scale bars, 100 μm. db, dorsal bud; vb, ventral bud; gt, gut tube..

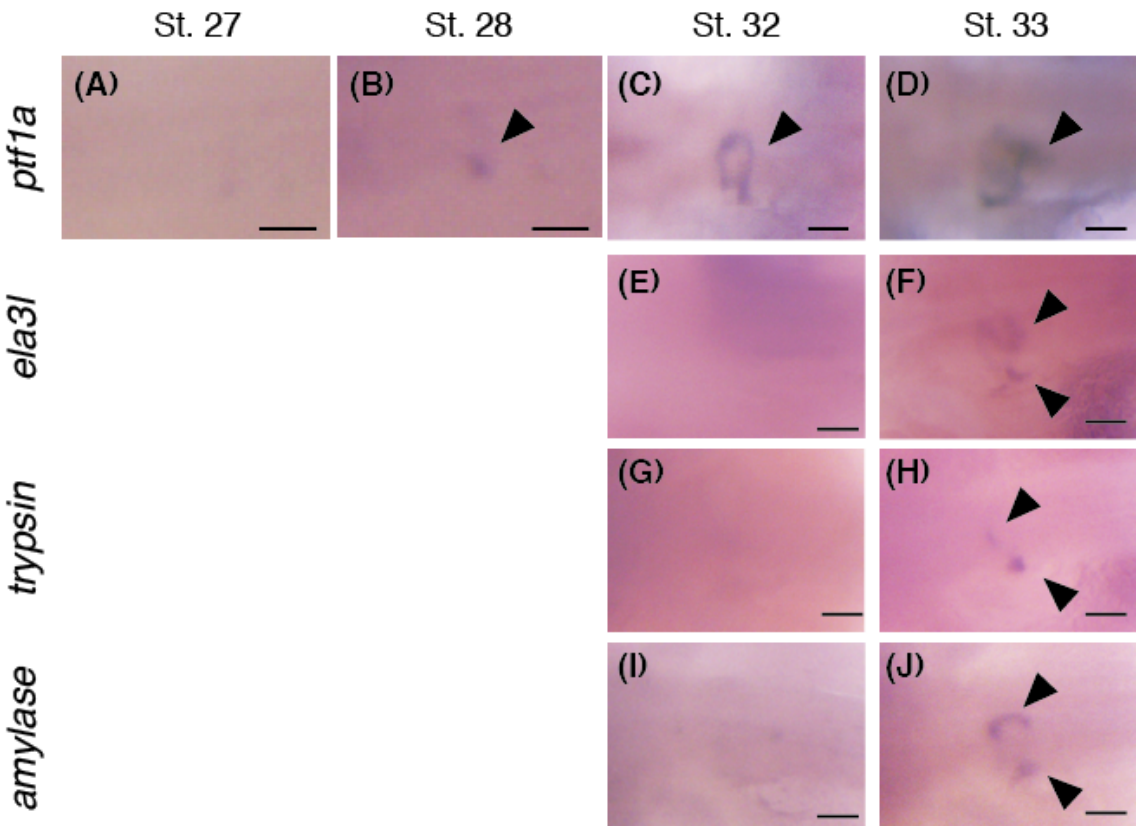

Fig. 9. Expression of exocrine cell markers

(A-J) *in situ* hybridization for *ptf1a* (A-D), *elastase 3* (E, F, *ela3l*), *trypsin* (G, H), *amylase* (I, J). *ptf1a* expression is detected from stage 28 in ventral bud (B, black arrowhead). This stage is consistent with the stage when the strong mCherry expression starts in the ptf1a-mCherry embryos. *ptf1a* expression is detected around the dorsal bud, and then expands along the gut tube (C, D, Fig. 6.). Exocrine marker genes, *ela3l*, *trypsin* and *amylase*, are all expressed from stage 33 in the *ptf1a*-expressing region (around the single principal islet region). All figures are in dorsal views, anterior to the left. Scale bars, 100 μm.

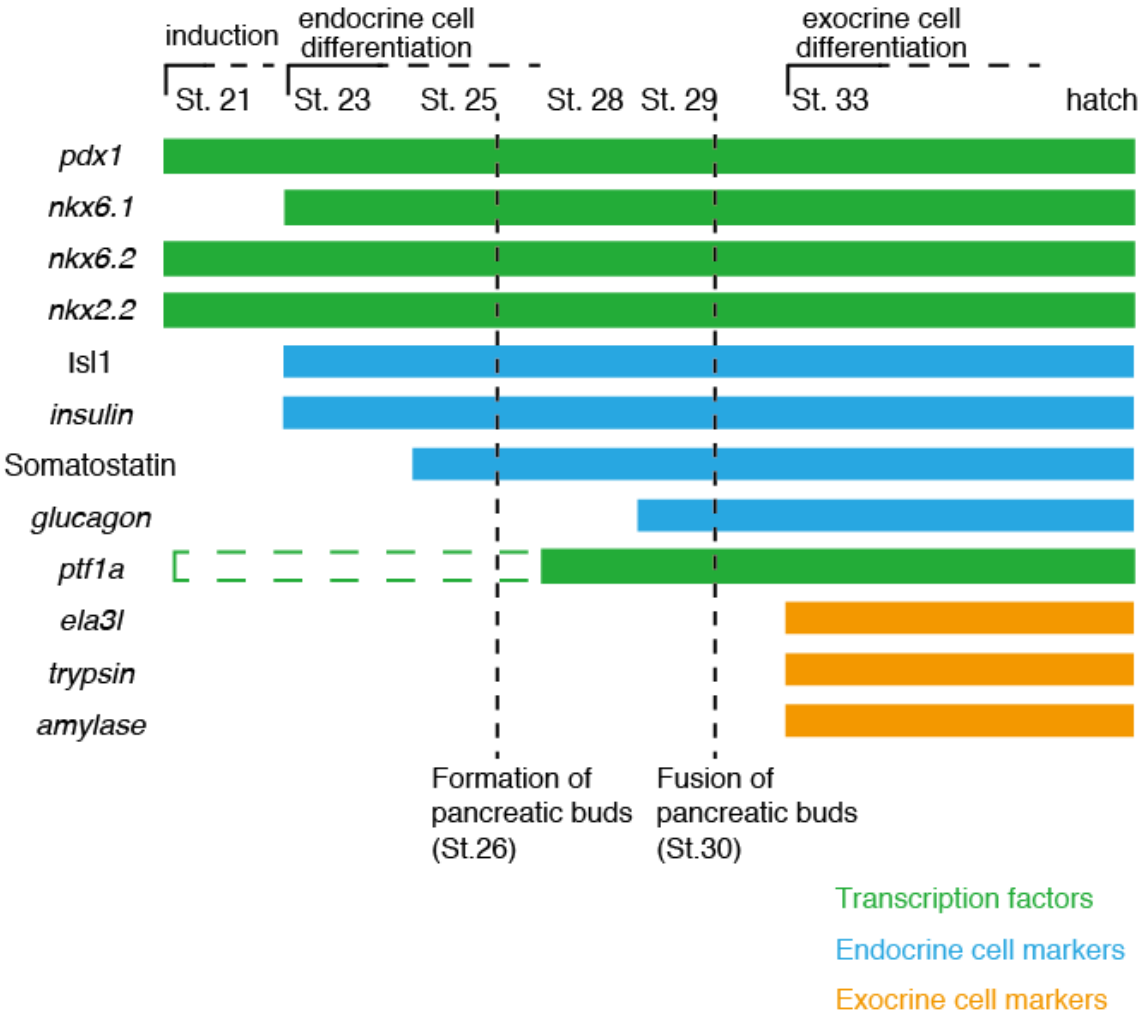

Fig. 10. Summary of expression timing during early pancreatic development in medaka

Chart shows the expression timing of endocrine- and exocrine- marker genes. A weak *ptf1a* expression is indicated as a dashed bar because it can be detected only in the *ptf1a-mCherry* Tg.

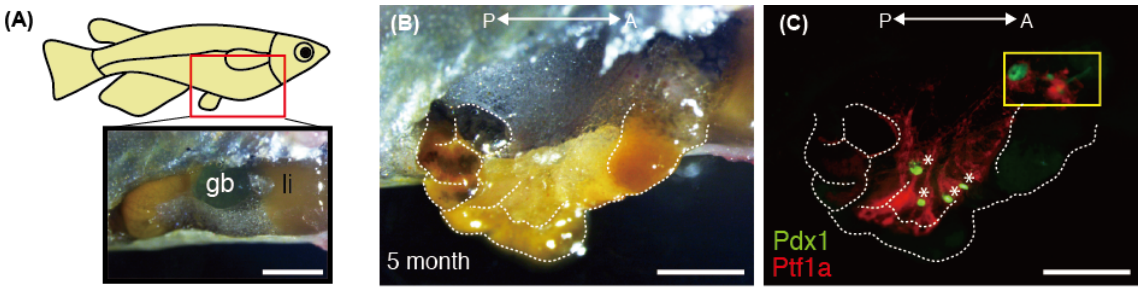

Fig. 11. Morphology of the adult pancreas in medaka

(A) Position of organs before extraction. Right side of the abdominal trunk region is opened (red square area). **(B, C)** Lateral view of the dissected internal organs. (B) Bright-field image and (C) fluorescent image. White dotted lines show a gut tube. Asterisks show autofluorescence. Islets are observed in the anterior region between the liver and gut tube (yellow square). Exocrine tissue has the multiple connections to the gut tube from anterior to posterior. Anterior to the right. Scale bars, 2 mm. gb, gallbladder; li, liver.

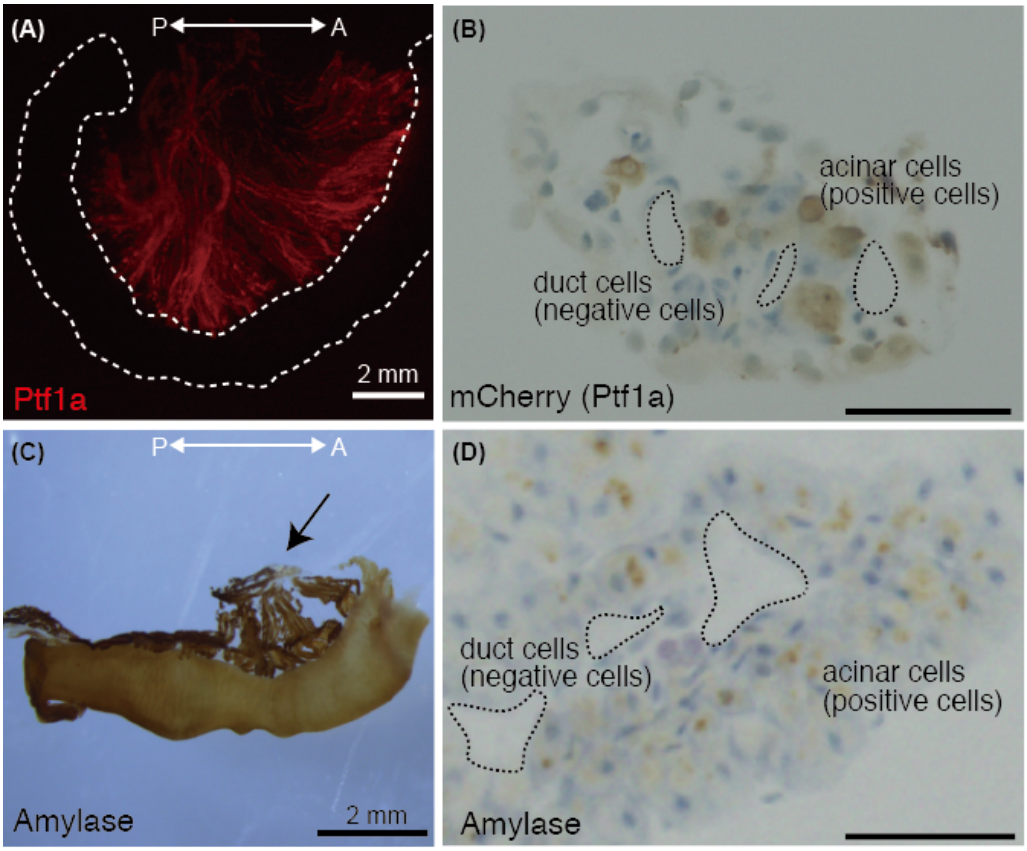

Fig. 12. Ductal structure in the mesentery

(A) Fluorescent image of a posterior gut tube of *ptf1a-mCherry* Tg fish. Exocrine cells exist within the mesentery and connect to the gut tube. White dotted lines show a gut tube. **(B)** Histological section of the mesentery of *ptf1a-mCherry* Tg fish stained with the anti-mCherry antibody. mCherry-positive cells (brown, putative acinar cells) and negative cells (putative duct cells) constitute the ductal structure. Dotted lines outline lumens of the ducts. **(C)** Immunohistochemistry of a posterior gut tube stained with the anti-Amylase antibody. Positive signals are observed in ductal structures within the mesentery

(arrow). **(D)** Histological section of the mesentery of panel C. Positive cells (brown, differentiated acinar cells) are present near ducts or between ducts, which is the similar distribution pattern of mCherry-positive cells in (B). Dotted lines outline lumens of the ducts. Anterior to the right in (A, C). Scale bars, 2 mm (A, C), 50 μm (B, D).

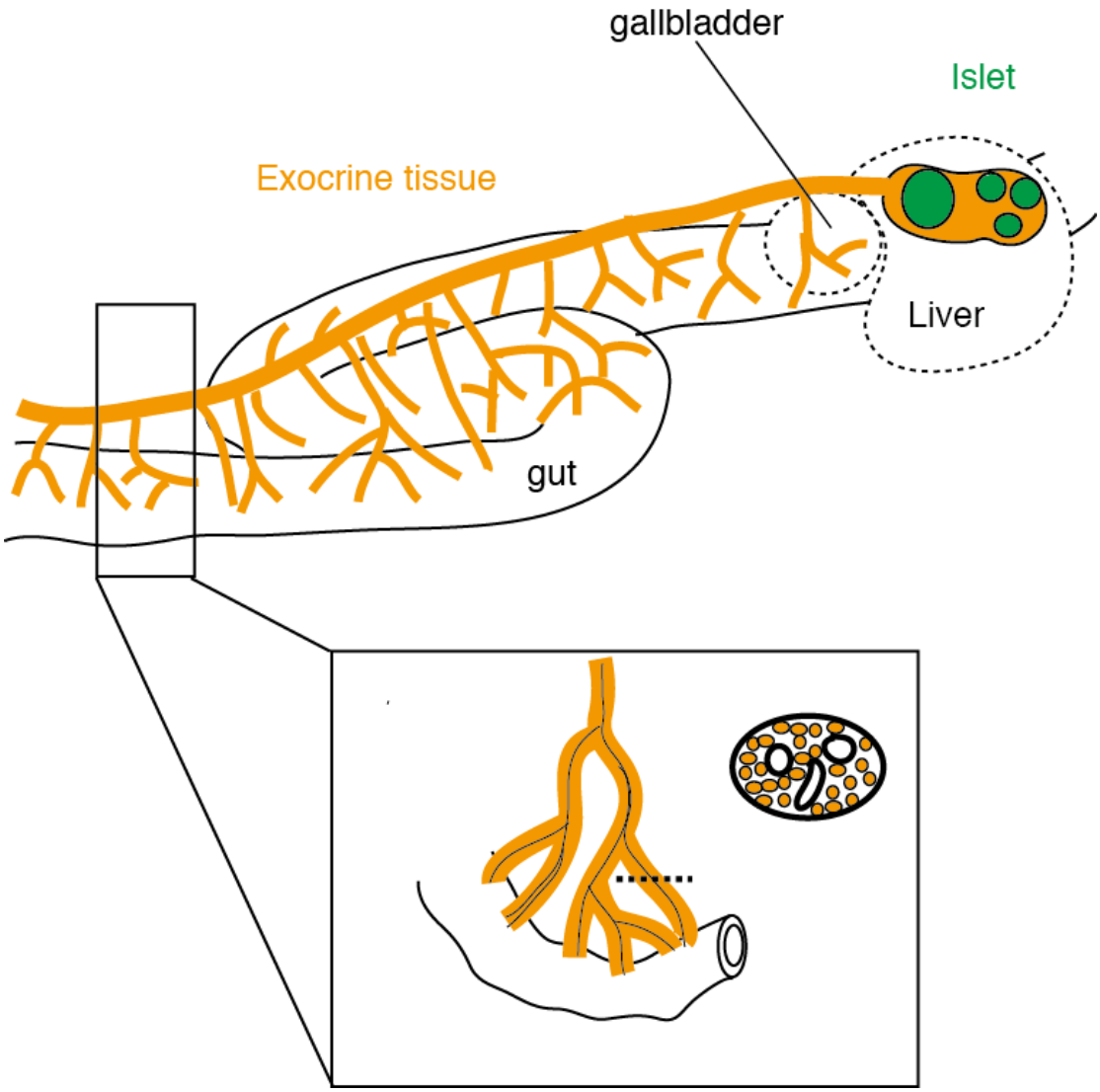

Fig. 13. The relationship between the adult pancreas and intestine in medaka

A schema of adult medaka pancreas to show the position of the islets (green) and the exocrine tissue (orange). Islets are located in between the liver and gut tube. The exocrine tissue expands broadly within the mesentery along the intestine. This exocrine tissue has multiple connections to the gut tube. Anterior to the right.

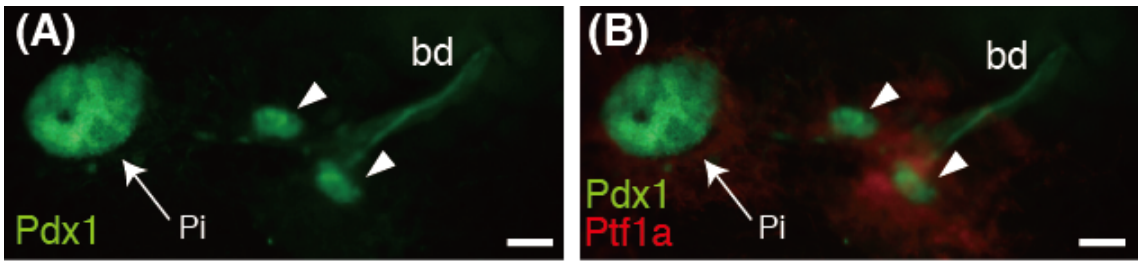

Fig. 14. Principal islet and secondary islets

(A, B) Fluorescent image of 5 months old double Tg fish showing Pdx1 and Ptf1a expression. (A) GFP fluorescent image, (B) GFP and mCherry fluorescent image. One big principal islet (Pi) derived from the dorsal bud (white arrows) and some small secondary islets are found at the extra principal islet region (white arrowheads). Exocrine cells surround principal and secondary islets. Anterior to the right. Scale bar, 100 μm. bd, bile duct; Pi, principal islet.

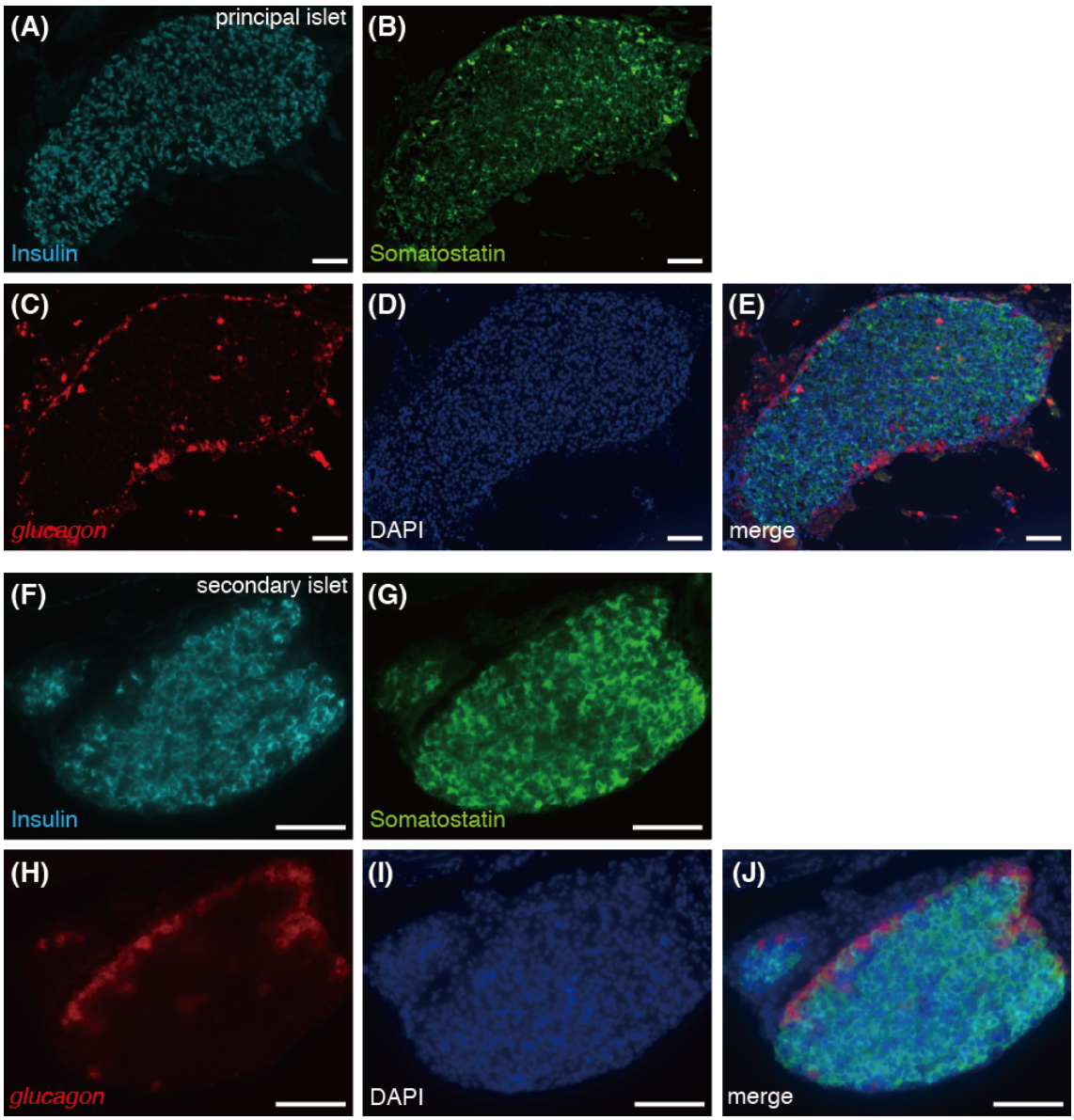

Fig. 15. The endocrine component of principal and secondary islets

(A, B, C, D, E) Section images of Insulin-producing cells (A), Somatostatin-producing cells (B), *glucagon*-producing cells (C), nuclear (D) and combination of all fluorescent images of a principal islet (E).

(F, G, H, I, J) Section images of Insulin-producing cells (F), Somatostatin-

producing cells (G), *glucagon*-producing cells (H), nuclear (I) and combination of all fluorescent images of secondary islets (J). Insulin-producing cells and Somatostatin-producing cells are located in the central of islets and *glucagon*-producing cells are in the periphery. Scale bars, 50 μm.

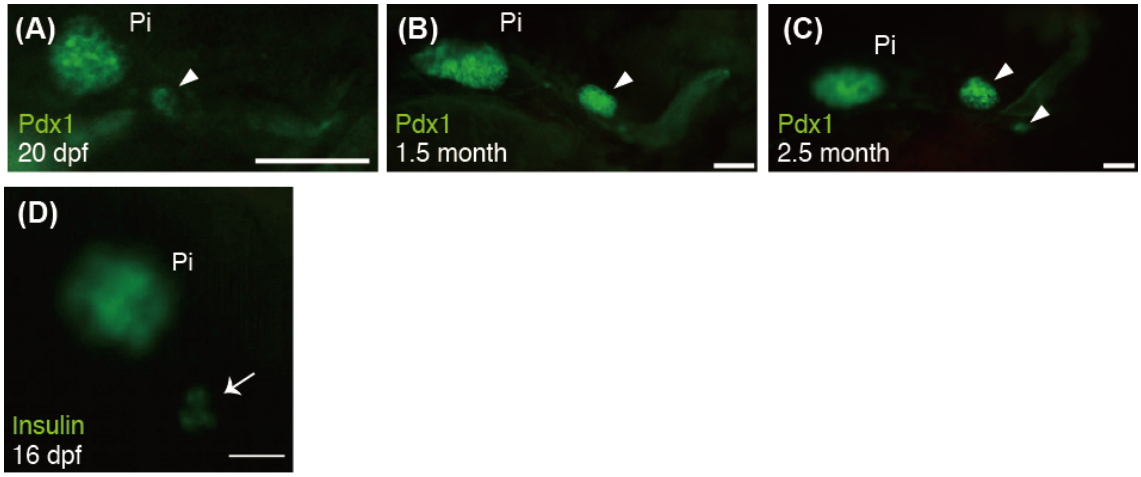

Fig. 16. The development of secondary islets after hatch

(A, B, C) Lateral view of dissected pancreases of 20 dpf (A), 1.5 mpf (B) and 2.5 mpf (C) *pdx1-EGFP* Tg fish. The number of secondary islets increased as fish grows (white arrowheads). (D) Lateral view of the dissected pancreas of 16 dpf *insulin-EGFP-NTR* Tg fish. First secondary islet appears extra principal islet region after hatch (white arrow). Pi, principal islet. Anterior to the right in all figures. Scale bars, 2 mm (A, B, C), 25 μm (D).

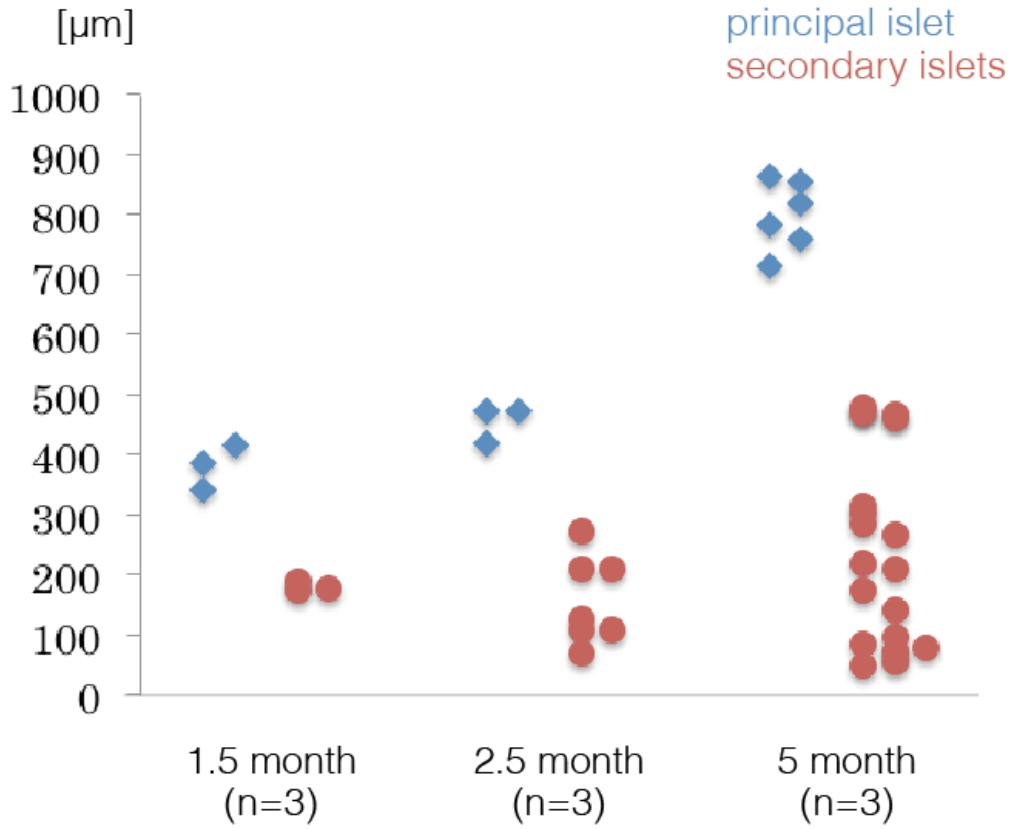

Fig. 17. The size of principal islet and secondary islets during growth

Scatter plot of the long axis length about principal islet and secondary islets. Y axis shows the long axis length of each islets. Both of principal and secondary islets gradually increased their size as they grow.

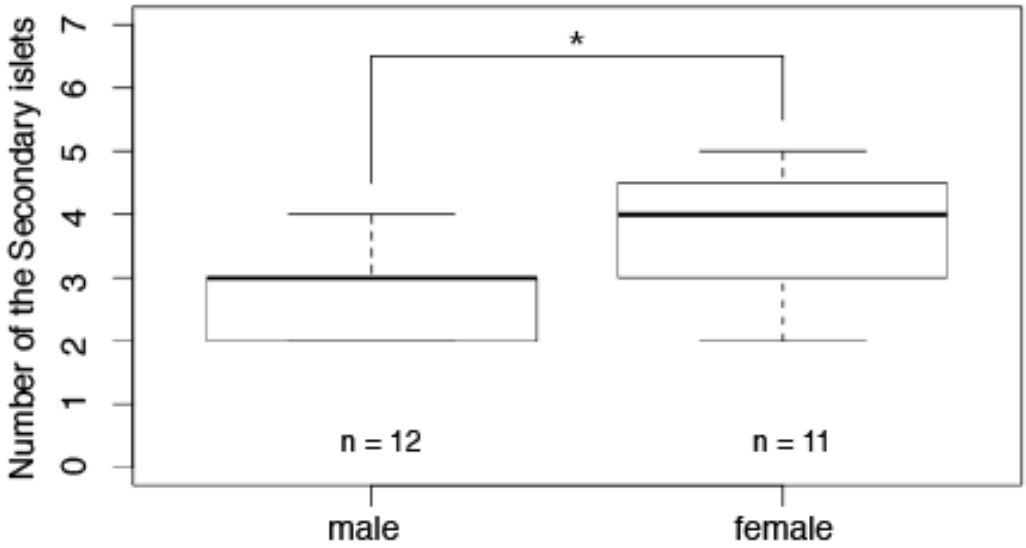

Fig. 18. Sex differences of secondary islets number.

Box plot comparing the number of secondary islets between males (n = 12) and females (n = 11) (*p = 0.024 by Mann-Whitney U test).

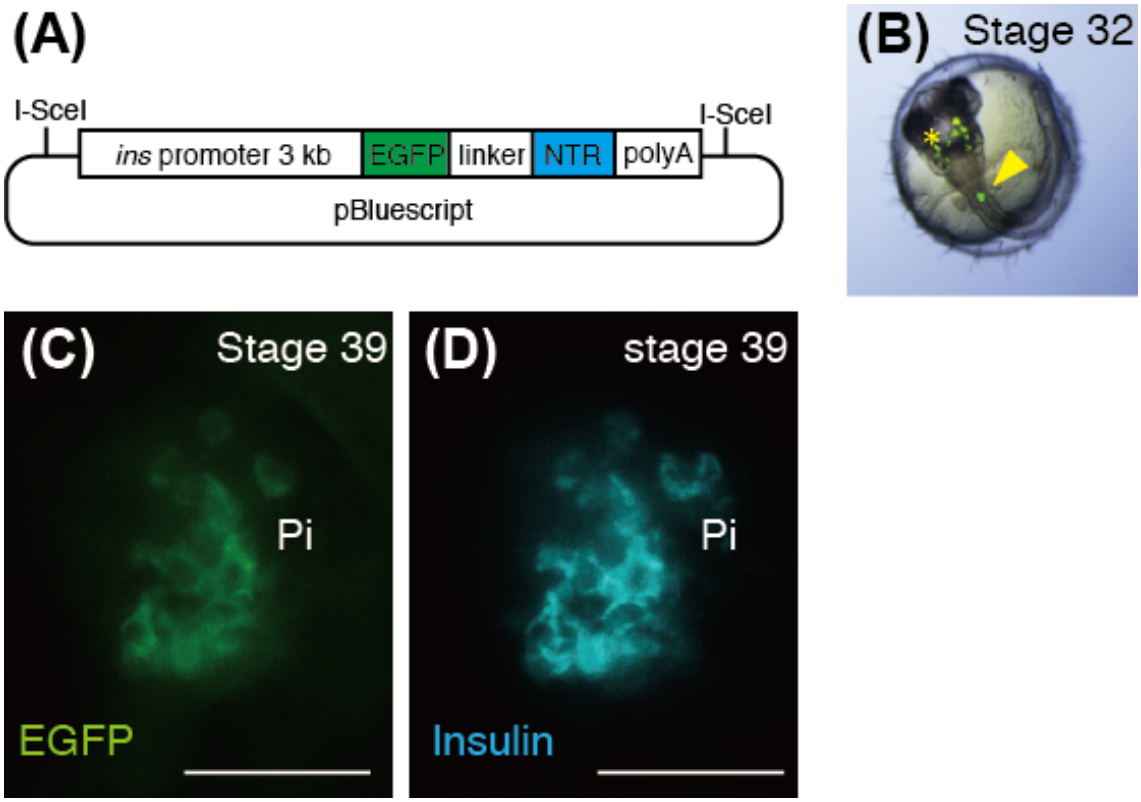

Fig. 19. Establishment of *insulin-GFP-NTR* Tg

(A) Schematic representation of the constructs used to drive β cell expression of the fusion protein GFP-NTR under the 3-kb insulin promoter region. **(B)** Fluorescent image of an *insulin-EGFP-NTR* Tg embryo at stage 32 showing GFP expression within the principal islet (yellow arrowhead). The asterisk shows autofluorescence. **(C, D)** Section images of EGFP (green) (C) and Insulin-producing cells (cyan, stained by the anti-Insulin antibody) (D) in a principal islet at stage 39 (hatching stage). EGFP signals are overlapped by endogenous Insulin signals. Pi, principal islet. Scale bars, 25 μm.

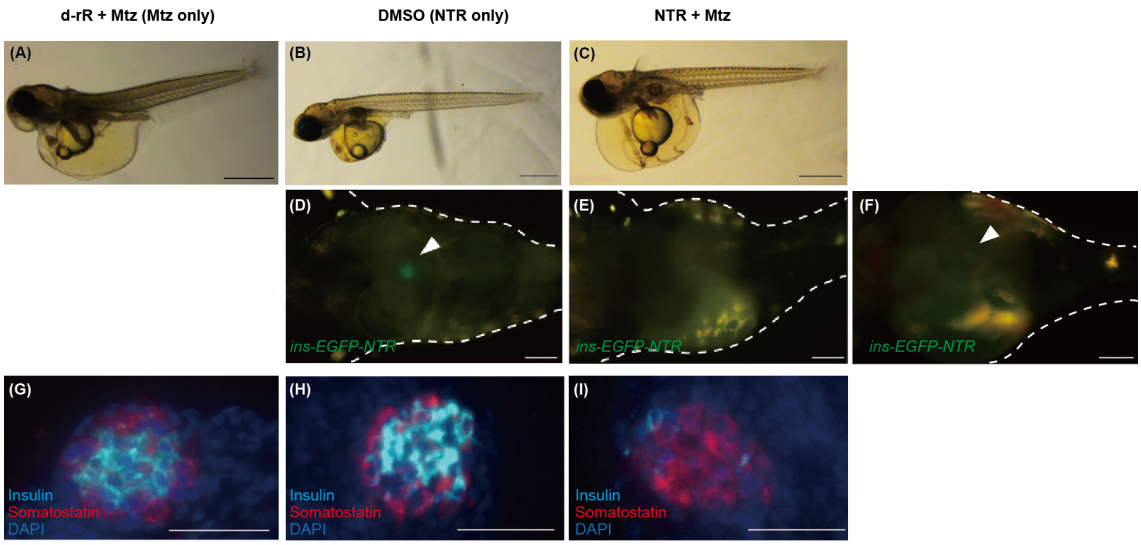

Fig. 20. Ablation of β cells by the NTR/Mtz system

(A-C) Bright field images of Mtz treated d-rR (A), DMSO treated Tg (B), and Mtz treated Tg fishes (C) just after washing out the prodrug. A part of the Mtz-treated group shows morphological changes. **(D-F)** Ventral view of the DMSO-treated Tg (D) and Mtz treated Tg (E, F) larva just after washing out the prodrug. The white dotted line indicates the body outline. About half of the Mtz-treated Tg fishes (15/27) lost fluorescence (E) and the other (12/27) show significant reduction in intensity of fluorescence (F). **(G-I)** Section images of principal islets in Mtz-treated d-rR (G), DMSO-treated Tg (H), and Mtz-treated Tg fishes (I). β cells were ablated only when the NTR/Mtz system worked. Scale bars, 2 mm (A-C), 200 μm (D-F), 50 μm (G-I).

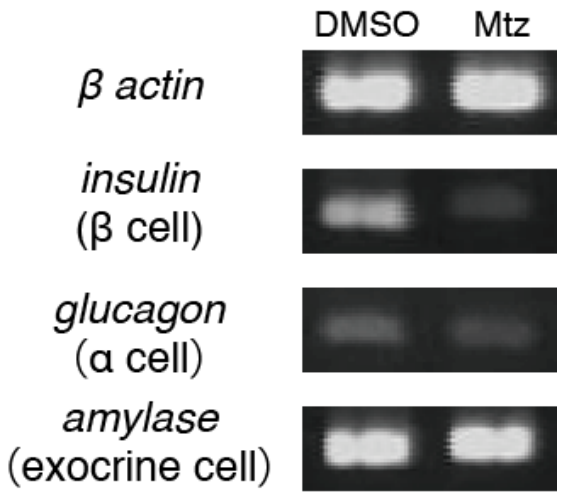

Fig. 21. RT-PCR of each marker genes

RT-PCR analysis of *insulin*, *glucagon*, *amylase*, and *β actin* expression in Mtz/DMSO-treated embryos.

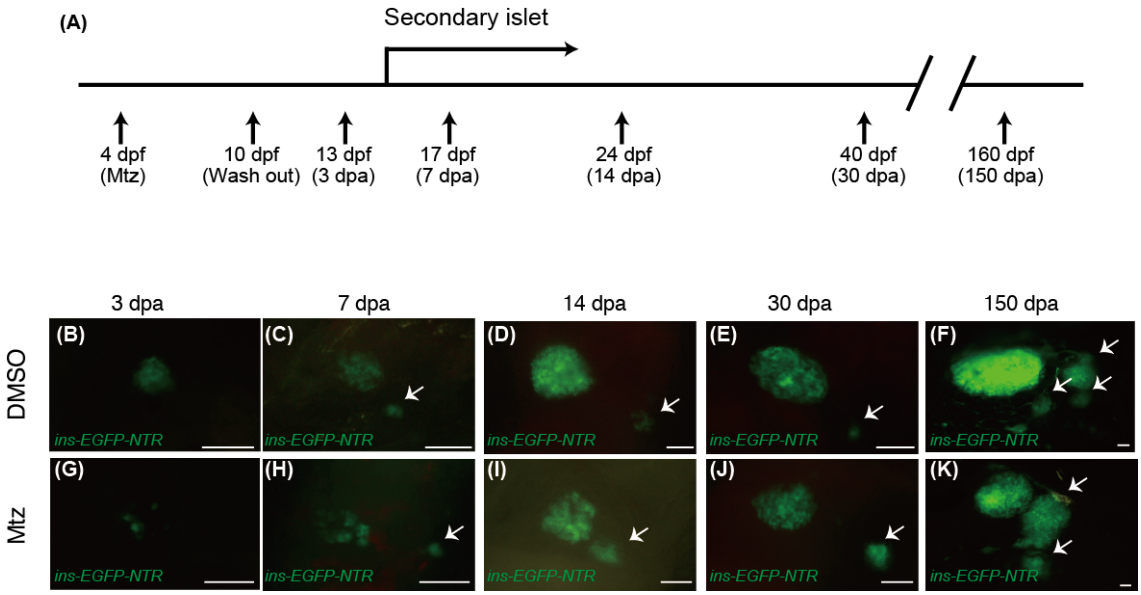

Fig. 22. β cell regeneration after Mtz/DMSO treatment

(A) Time course of Mtz treatment and observation. **(B-F)** Lateral view of the dissected pancreas of 3 dpa (B), 7 dpa (C), 14 dpa (D), 30 dpa (E) and 150 dpa (F) DMSO treated *insulin-EGFP-NTR*-Tg fishes. **(G-K)** Lateral view of the dissected pancreas of 3 dpa (G), 7 dpa (H), 14 dpa (I), 30 dpa (J) and 150 dpa (K) Mtz prodrug treated *insulin-EGFP-NTR*-Tg fishes. The white arrow shows the secondary islets. Anterior to the right. Scale bars, 100 μm.

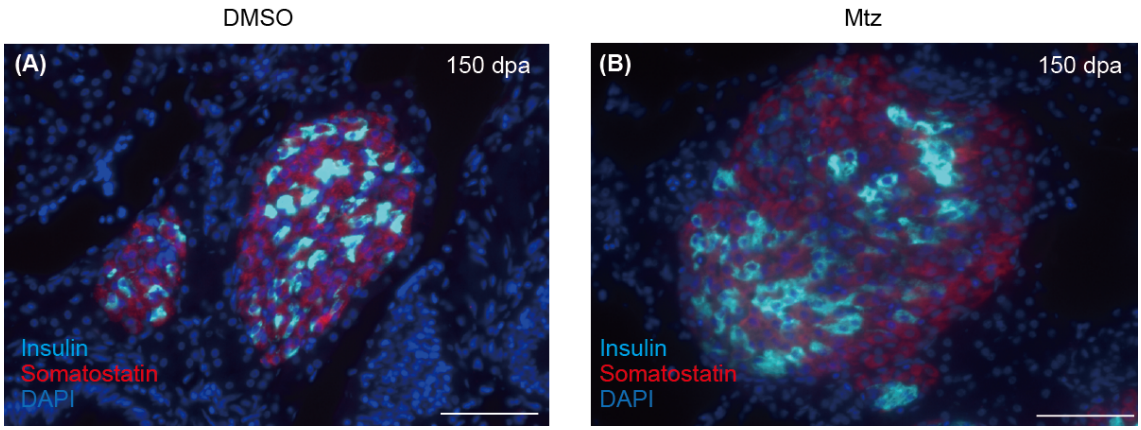

Fig. 23. Cell component of secondary islets after β cell ablation in principal islets

(A, B) Section images of secondary islets in DMSO-treated Tg (A) and Mtz-treated Tg (B) at 150 dpa. Mtz-treated Tg fishes tend to have larger secondary islets, but the cell component does not change. Scale bars, 50 μm.

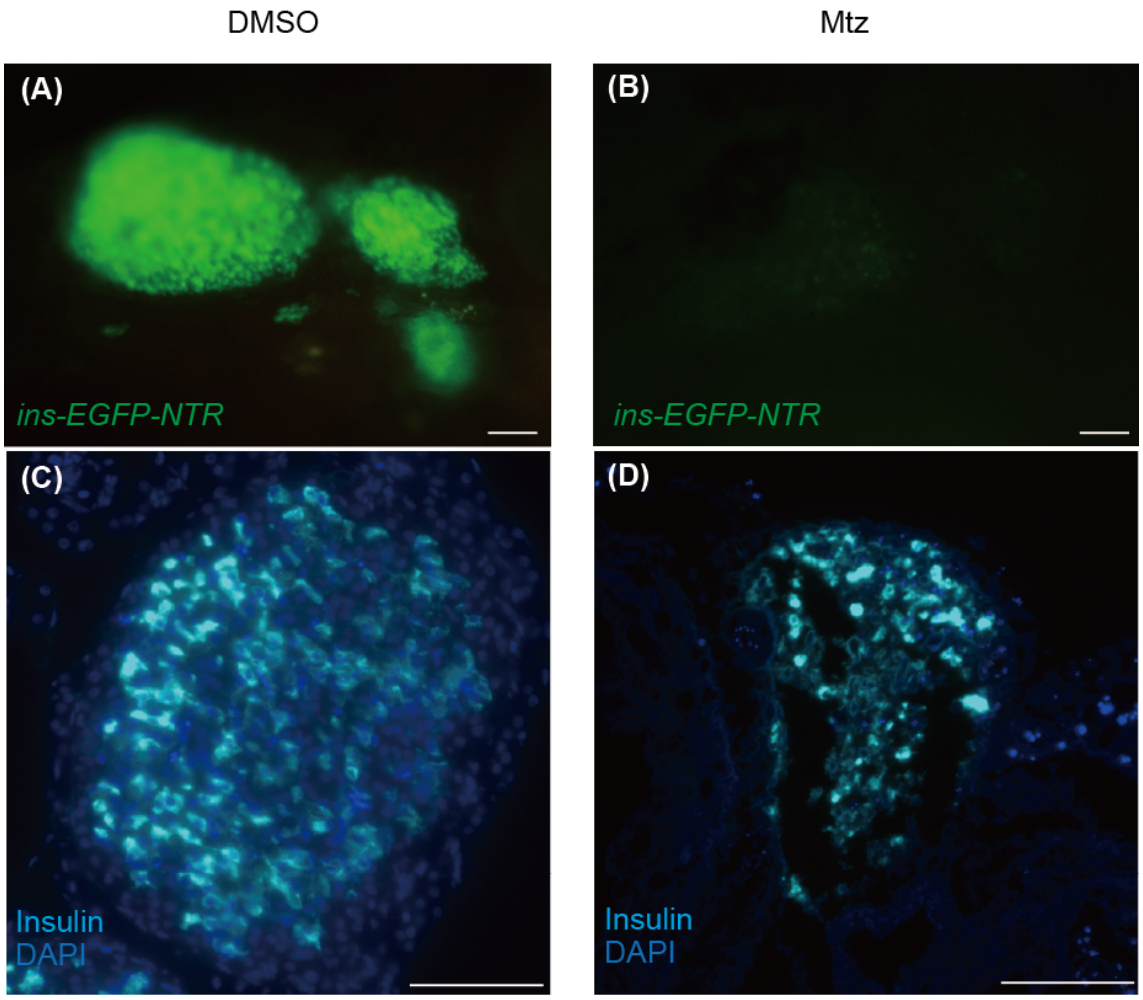

Fig. 24. β cell ablation via Mtz treatment in adult stage

(A, B) Lateral view of dissected pancreases of DMSO-injected (A) and Mtz-injected (B) Tg fishes. Significant loss of GFP signals was observed. **(C, D)** Section images of islet in DMSO-injected (C) and Mtz-injected (B) fishes. In the Mtz-injected Tg fish, the islet structure was disrupted. Anterior to the right (A, B). Scale bars, 100 μm (A, B), 50 μm (C, D).

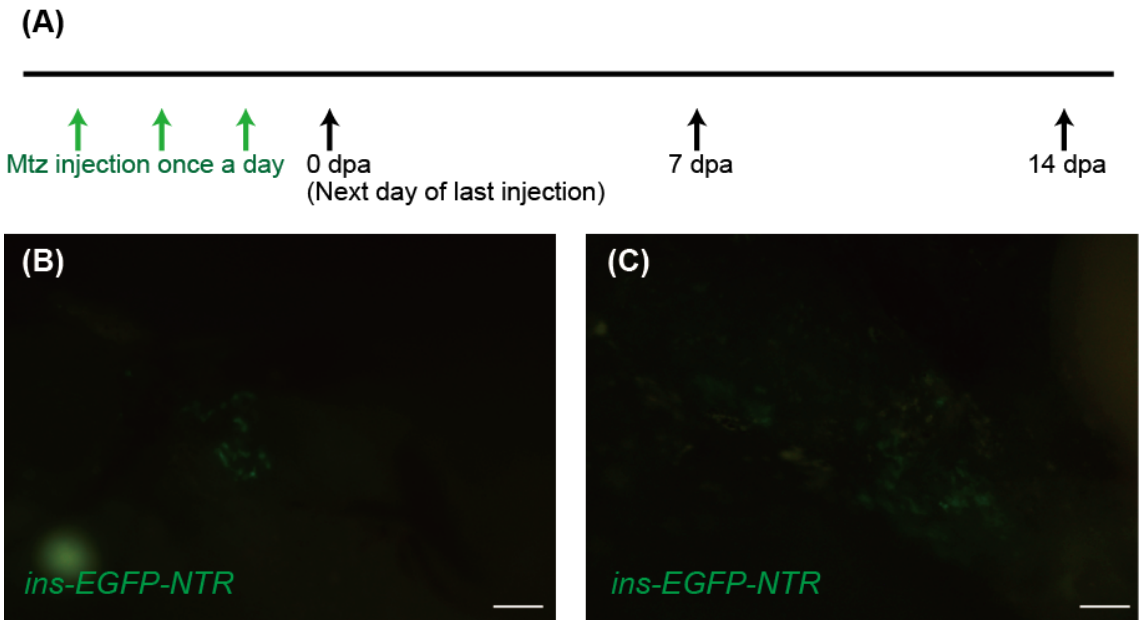

Fig. 25. β cell regeneration in adult stage

(A) Time course of Mtz injection and observation. **(B, C)** Lateral view of the dissected pancreases of Mtz-injected Tg fish at 7 dpa (B) and 14 dpa (C). GFP signal was slightly increased after ablation, but it did not recover well. Anterior to the right. Scale bars, 100 μm.

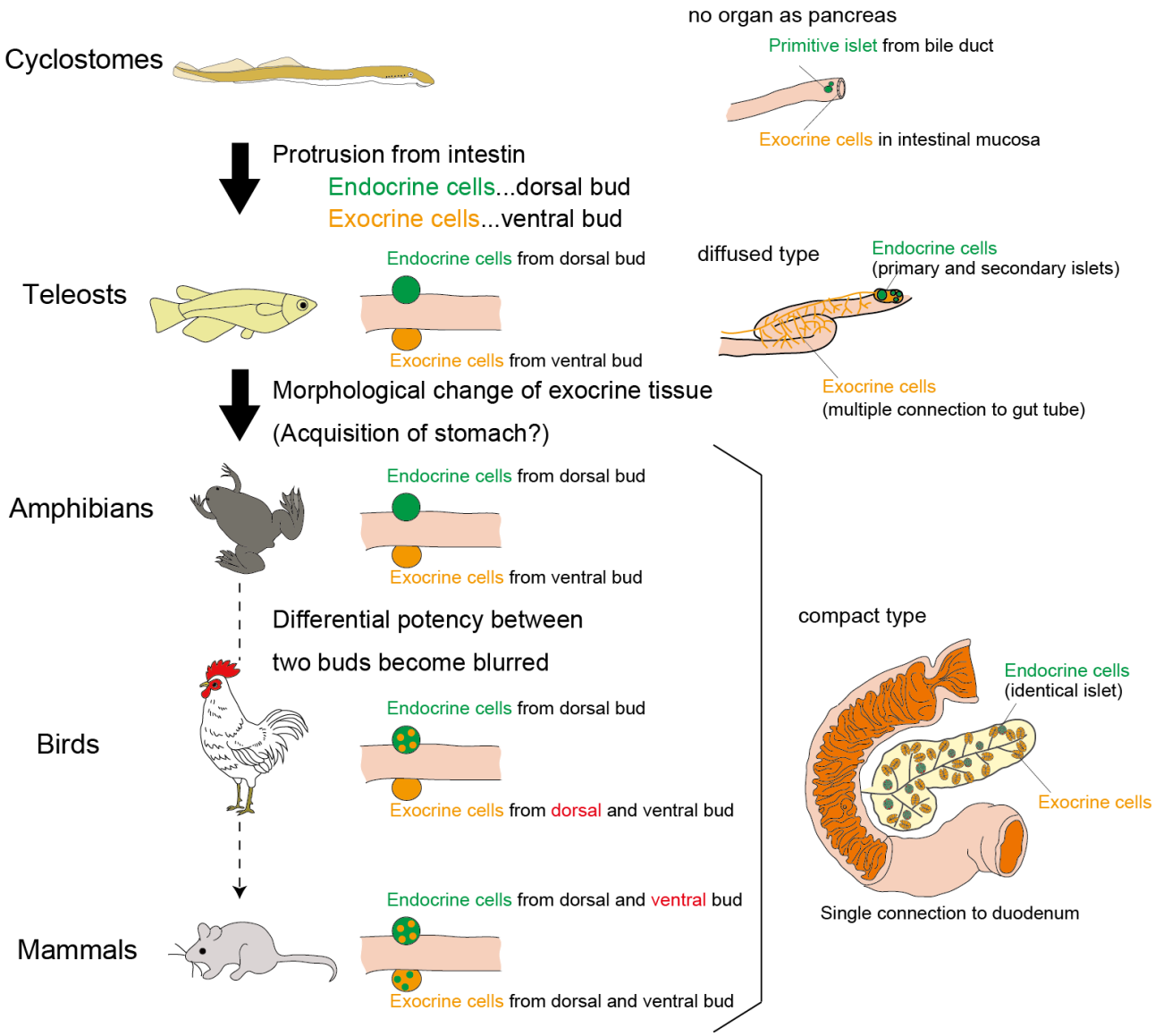

Fig. 26. The hypothesis of pancreas evolution

The evolutionally scenario of the development of the pancreas from cyclostomes to mammals. First, endocrine cells and exocrine cells developed independently (cyclostomes). Then the region of exocrine and endocrine cell development

becomes restricted into the anterior of the gut tube, according to functional and morphological changes of the intestine. The two types of cells are derived from two buds and fuse to make a diffused-type pancreas (Teleosts). A big morphological change occurred by the acquisition of stomach in amphibians, and pancreas acquired a compact shape. This compact type of pancreas is conserved to mammals. The difference in differentiation potency between the two buds gradually becomes blurred as vertebrates evolved to mammals.

Tables

Table 1. Gene-specific primers used for probe synthesis

Gene	5' primer (5' to 3')	3' primer (5' to 3')
pdx1	ATGAACCGGGAAGATCATTACTACCC	CTATGCTGGTTCTCTTGTCACAGACG
nkx6.1	TCTTCTGGCCGGGAGTCATG	AAGTGCTTTACATGAAGCTGCG
nkx6.2	ATGGAAGCTAACCGGCAGAG	CACTTGGTCCTCCGGTTCTG
insulin	GGCAGCTCTGTGGCTTCAGACATT	TGCATGGCTTGTGGCAGCACT
glucagon	TGGACTTCTGCTCCTCATCC	CAGCCAGGACACAAACTCCT
ptf1a	ATGGACTCTGTTCTAGACCCTTTCTCT	TCAAGCCACCAGGCCAAAAG
ela3l	GCTAGTGCCCTTGGGTGCGG	GCTGGCAATGCCGTGGACCT
trypsin	TCTCCTAGCCCTTTGTGCTG	CAGAGACACGGTGCTCACAT
amylase	GTGAGCAGTCCTTGGAGACC	TAATGGGCTCACCTCCGAGA
gfp	GACGTAAACGGCCACAAGTT	GAACTCCAGCAGGACCATGT
mCherry	CCATCATCAAGGAGTTCATGC	CATGGTCTTCTTCTGCATTACG

Table 2. Gene-specific primers used for qPCR

Gene	5’ primer (5’ to 3’)	3’ primer (5’ to 3’)
Insulin	GGCAGCTCTGTGGCTTCAGACATT	TGCATGGCTTGTGGCAGCACT
glucagon	TGGACTTCTGCTCCTCATCC	CAGCCAGGACACAAACTCCT
amylase	GTGAGCAGTCCTTGGAGACC	TAATGGGCTCACCTCCGAGA
β actin	GATGAAGCCCAGAGCAAGAG	AGGAAGGAAGGCTGGAAGAG

References

Ahlgren, U., Pfaff, S. L., Jessell, T. M., Edlund, T. & Edlund, H. 1997. Independent requirement for ISL1 in formation of pancreatic mesenchyme and islet cells. *Nature,* **385,** 257-260.

Ahnfelt-Rønne, J., Jørgensen, M. C., Hald, J., Madsen, O. D., Serup, P. & Hecksher-Sørensen, J. 2007. An improved method for three-dimensional reconstruction of protein expression patterns in intact mouse and chicken embryos and organs. *J Histochem Cytochem,* **55,** 925-930.

Anlezark, G. M., Melton, R. G., Sherwood, R. F., Coles, B., Friedlos, F. & Knox, R. J. 1992. The bioactivation of 5-(aziridin-1-yl)-2,4-dinitrobenzamide (CB1954)--I. Purification and properties of a nitroreductase enzyme from Escherichia coli--a potential enzyme for antibody-directed enzyme prodrug therapy (ADEPT). *Biochem Pharmacol,* **44,** 2289-2295.

Argenton, F., Zecchin, E. & Bortolussi, M. 1999. Early appearance of pancreatic hormone-expressing cells in the zebrafish embryo. *Mech Dev,* **87,** 217-221.

Assouline, B., Nguyen, V., Mahé, S., Bourrat, F. & Scharfmann, R. 2002. Development of the pancreas in medaka. *Mech Dev,* **117,** 299-303.

Ben-Othman, N., Courtney, M., Vieira, A. et al. 2013. From pancreatic islet formation to beta-cell regeneration. *Diabetes Res Clin Pract,* **101,** 1-9.

Binot, A. C., Manfroid, I., Flasse, L. et al. 2010. Nkx6.1 and nkx6.2 regulate alpha- and beta-cell formation in zebrafish by acting on pancreatic endocrine progenitor cells. *Dev Biol,* **340,** 397-407.

Burlison, J. S., Long, Q., Fujitani, Y., Wright, C. V. & Magnuson, M. A. 2008. Pdx-1 and Ptf1a concurrently determine fate specification of pancreatic multipotent progenitor cells. *Dev Biol,* **316,** 74-86.

Castro, L. F., Gonçalves, O., Mazan, S., Tay, B. H., Venkatesh, B. & Wilson, J. M. 2014. Recurrent gene loss correlates with the evolution of stomach phenotypes in gnathostome history. *Proc Biol Sci,* **281,** 20132669.

Chakrabarti, S. K., James, J. C. & Mirmira, R. G. 2002. Quantitative assessment of gene targeting in vitro and in vivo by the pancreatic transcription factor, Pdx1. Importance of chromatin structure in directing promoter binding. *J Biol Chem,* **277,** 13286-13293.

Curado, S., Anderson, R. M., Jungblut, B., Mumm, J., Schroeter, E. & Stainier, D. Y. 2007. Conditional targeted cell ablation in zebrafish: a new tool for regeneration studies. *Dev Dyn,* **236,** 1025-1035.

Desgraz, R., Bonal, C. & Herrera, P. L. 2011. β-cell regeneration: the pancreatic intrinsic faculty. *Trends Endocrinol Metab,* **22,** 34-43.

Desgraz, R. & Herrera, P. L. 2009. Pancreatic neurogenin 3-expressing cells are unipotent islet precursors. *Development,* **136,** 3567-3574.

Dong, P. D., Provost, E., Leach, S. D. & Stainier, D. Y. 2008. Graded levels of Ptf1a differentially regulate endocrine and exocrine fates in the developing pancreas. *Genes Dev,* **22,** 1445-1450.

Dor, Y., Brown, J., Martinez, O. I. & Melton, D. A. 2004. Adult pancreatic beta-cells are formed by self-duplication rather than stem-cell differentiation. *Nature,* **429,** 41-46.

Du, A., Hunter, C. S., Murray, J. et al. 2009. Islet-1 is required for the maturation, proliferation, and survival of the endocrine pancreas. *Diabetes,* **58,** 2059-2069.

Edwards, D. I. 1993. Nitroimidazole drugs--action and resistance mechanisms. II. Mechanisms of resistance. *J Antimicrob Chemother,* **31,** 201-210.

Epple, A. & Brinn, J. E. 1975. Islet histophysiology: evolutionary correlations. *Gen Comp Endocrinol,* **27,** 320-349.

Field, H. A., Dong, P. D., Beis, D. & Stainier, D. Y. 2003. Formation of the digestive system in zebrafish. II. Pancreas morphogenesis. *Dev Biol,* **261,** 197-208.

Furutani-Seiki, M., Sasado, T., Morinaga, C. et al. 2004. A systematic genome-wide screen for mutations affecting organogenesis in Medaka, Oryzias latipes. *Mech Dev,* **121,** 647-658.

Gemberling, M., Bailey, T. J., Hyde, D. R. & Poss, K. D. 2013. The zebrafish as a model for complex tissue regeneration. *Trends Genet,* **29,** 611-620.

Godinho, L., Mumm, J. S., Williams, P. R. et al. 2005. Targeting of amacrine cell neurites to appropriate synaptic laminae in the developing zebrafish retina. *Development,* **132,** 5069-5079.

Guz, Y., Montminy, M. R., Stein, R. et al. 1995. Expression of murine STF-1, a putative insulin gene transcription factor, in beta cells of pancreas, duodenal epithelium and pancreatic exocrine and endocrine progenitors during ontogeny. *Development,* **121,** 11-18.

Guz, Y., Nasir, I. & Teitelman, G. 2001. Regeneration of pancreatic beta cells from intra-islet precursor cells in an experimental model of diabetes. *Endocrinology,* **142,** 4956-4968.

Hesselson, D., Anderson, R. M. & Stainier, D. Y. 2011. Suppression of Ptf1a activity induces acinar-to-endocrine conversion. *Curr Biol,* **21,** 712-717.

Horb, M. E. & Slack, J. M. 2002. Expression of amylase and other pancreatic genes in Xenopus. *Mech Dev,* **113,** 153-157.

Hoshino, M., Nakamura, S., Mori, K. et al. 2005. Ptf1a, a bHLH transcriptional gene,

defines GABAergic neuronal fates in cerebellum. *Neuron,* **47,** 201-213.

Huang, H., Vogel, S. S., Liu, N., Melton, D. A. & Lin, S. 2001. Analysis of pancreatic development in living transgenic zebrafish embryos. *Mol Cell Endocrinol,* **177,** 117-124.

Incardona, J. P., Collier, T. K. & Scholz, N. L. 2004. Defects in cardiac function precede morphological abnormalities in fish embryos exposed to polycyclic aromatic hydrocarbons. *Toxicol Appl Pharmacol,* **196,** 191-205.

Ishikawa, Y. 2000. Medakafish as a model system for vertebrate developmental genetics. *Bioessays,* **22,** 487-495.

Iwamatsu, T. 2004. Stages of normal development in the medaka Oryzias latipes. *Mech Dev,* **121,** 605-618.

Jensen, J. 2004. Gene regulatory factors in pancreatic development. *Dev Dyn,* **229,** 176-200.

Jonsson, J., Carlsson, L., Edlund, T. & Edlund, H. 1994. Insulin-promoter-factor 1 is required for pancreas development in mice. *Nature,* **371,** 606-609.

Jørgensen, M. C., Ahnfelt-Rønne, J., Hald, J., Madsen, O. D., Serup, P. & Hecksher-Sørensen, J. 2007. An illustrated review of early pancreas development in the mouse. *Endocr Rev,* **28,** 685-705.

Karlsson, O., Thor, S., Norberg, T., Ohlsson, H. & Edlund, T. 1990. Insulin gene enhancer binding protein Isl-1 is a member of a novel class of proteins containing both a homeo- and a Cys-His domain. *Nature,* **344,** 879-882.

Kasahara, M., Naruse, K., Sasaki, S. et al. 2007. The medaka draft genome and insights into vertebrate genome evolution. *Nature,* **447,** 714-719.

Katogi, R., Nakatani, Y., Shin-I, T., Kohara, Y., Inohaya, K. & Kudo, A. 2004. Large-scale analysis of the genes involved in fin regeneration and blastema formation in the medaka, Oryzias latipes. *Mech Dev,* **121,** 861-872.

Katsuyama, T. & Paro, R. 2011. Epigenetic reprogramming during tissue regeneration. *FEBS Lett,* **585,** 1617-1624.

Kawaguchi, Y., Cooper, B., Gannon, M., Ray, M., Macdonald, R. J. & Wright, C. V. 2002. The role of the transcriptional regulator Ptf1a in converting intestinal to pancreatic progenitors. *Nat Genet,* **32,** 128-134.

Kawakami, A., Fukazawa, T. & Takeda, H. 2004. Early fin primordia of zebrafish larvae regenerate by a similar growth control mechanism with adult regeneration. *Dev Dyn,* **231,** 693-699.

Kelsh, R. N., Inoue, C., Momoi, A. et al. 2004. The Tomita collection of medaka pigmentation mutants as a resource for understanding neural crest cell development. *Mech Dev,* **121,** 841-859.

Kim, H. J., Sumanas, S., Palencia-Desai, S., Dong, Y., Chen, J. N. & Lin, S. 2006. Genetic analysis of early endocrine pancreas formation in zebrafish. *Mol Endocrinol,* **20,** 194-203.

Kimura, T., Jindo, T., Narita, T. et al. 2004. Large-scale isolation of ESTs from medaka embryos and its application to medaka developmental genetics. *Mech Dev,* **121,** 915-932.

Krapp, A., Knöfler, M., Ledermann, B. et al. 1998. The bHLH protein PTF1-p48 is essential for the formation of the exocrine and the correct spatial organization of the endocrine pancreas. *Genes Dev,* **12,** 3752-3763.

Li, Z., Wen, C., Peng, J., Korzh, V. & Gong, Z. 2009. Generation of living color transgenic zebrafish to trace somatostatin-expressing cells and endocrine

pancreas organization. *Differentiation,* **77,** 128-134.

Lindmark, D. G. & Müller, M. 1976. Antitrichomonad action, mutagenicity, and reduction of metronidazole and other nitroimidazoles. *Antimicrob Agents Chemother,* **10,** 476-482.

Loosli, F., Köster, R. W., Carl, M. et al. 2000. A genetic screen for mutations affecting embryonic development in medaka fish (Oryzias latipes). *Mech Dev,* **97,** 133-139.

Matsuura, K., Katsumoto, K., Fukuda, K., Kume, K. & Kume, S. 2009. Conserved origin of the ventral pancreas in chicken. *Mech Dev,* **126,** 817-827.

Moriyama, Y., Kawanishi, T., Nakamura, R. et al. 2012. The medaka zic1/zic4 mutant provides molecular insights into teleost caudal fin evolution. *Curr Biol,* **22,** 601-607.

Moss, J. B., Koustubhan, P., Greenman, M., Parsons, M. J., Walter, I. & Moss, L. G. 2009. Regeneration of the pancreas in adult zebrafish. *Diabetes,* **58,** 1844-1851.

Nakamura, R., Tsukahara, T., Qu, W. et al. 2014. Large hypomethylated domains serve as strong repressive machinery for key developmental genes in vertebrates. *Development,* **141,** 2568-2580.

Nakamura, S., Saito, D. & Tanaka, M. 2008. Generation of transgenic medaka using modified bacterial artificial chromosome. *Dev Growth Differ,* **50,** 415-419.

Nilsson, A. & Fänge, R. 1970. Digestive proteases in the cyclostome Myxine glutinosa (L). *Comp Biochem Physiol,* **32,** 237-250.

Offield, M. F., Jetton, T. L., Labosky, P. A. et al. 1996. PDX-1 is required for pancreatic outgrowth and differentiation of the rostral duodenum. *Development,* **122,** 983-995.

Ostberg, Y., Noorden, S. V. & Pearse, A. G. 1975. Cytochemical, immunofluorescence, and ultrastructural investigations on polypeptide hormone localization in the islet parenchyma and bile duct mucosa of a cyclostome, Myxine glutinosa. *Gen Comp Endocrinol,* **25,** 274-291.

Ostberg, Y., Van Noorden, S., Pearse, A. G. & Thomas, N. W. 1976. Cytochemical, immunofluorescence, and ultrastructural investigations on polypeptide hormone containing cells in the intestinal mucosa of a cyclostome, Myxine glutinosa. *Gen Comp Endocrinol,* **28,** 213-227.

Otsuka, T., Tsukahara, T. & Takeda, H. 2015. Development of the pancreas in medaka, Oryzias latipes, from embryo to adult. *Dev Growth Differ,* **57,** 557-569.

Pearl, E. J., Bilogan, C. K., Mukhi, S., Brown, D. D. & Horb, M. E. 2009. Xenopus pancreas development. *Dev Dyn,* **238,** 1271-1286.

Peshavaria, M., Larmie, B. L., Lausier, J. et al. 2006. Regulation of pancreatic beta-cell regeneration in the normoglycemic 60% partial-pancreatectomy mouse. *Diabetes,* **55,** 3289-3298.

Pisharath, H., Rhee, J. M., Swanson, M. A., Leach, S. D. & Parsons, M. J. 2007. Targeted ablation of beta cells in the embryonic zebrafish pancreas using E. coli nitroreductase. *Mech Dev,* **124,** 218-229.

Redd, M. J., Cooper, L., Wood, W., Stramer, B. & Martin, P. 2004. Wound healing and inflammation: embryos reveal the way to perfect repair. *Philos Trans R Soc Lond B Biol Sci,* **359,** 777-784.

Rembold, M., Lahiri, K., Foulkes, N. S. & Wittbrodt, J. 2006. Transgenesis in fish: efficient selection of transgenic fish by co-injection with a fluorescent reporter construct. *Nat Protoc,* **1,** 1133-1139.

Ridgway, D., Manas, D., Shaw, J. & White, S. 2010. Preservation of the donor pancreas

for whole pancreas and islet transplantation. *Clin Transplant,* **24,** 1-19.

Rood, P. P., Bottino, R., Balamurugan, A. N., Fan, Y., Cooper, D. K. & Trucco, M. 2006. Facilitating physiologic self-regeneration: a step beyond islet cell replacement. *Pharm Res,* **23,** 227-242.

Sander, M., Sussel, L., Conners, J. et al. 2000. Homeobox gene Nkx6.1 lies downstream of Nkx2.2 in the major pathway of beta-cell formation in the pancreas. *Development,* **127,** 5533-5540.

Sekimizu, K., Tagawa, M. & Takeda, H. 2007. Defective fin regeneration in medaka fish (Oryzias latipes) with hypothyroidism. *Zoolog Sci,* **24,** 693-699.

Slack, J. M. 1995. Developmental biology of the pancreas. *Development,* **121,** 1569-1580.

Sussel, L., Kalamaras, J., Hartigan-O'connor, D. J. et al. 1998. Mice lacking the homeodomain transcription factor Nkx2.2 have diabetes due to arrested differentiation of pancreatic beta cells. *Development,* **125,** 2213-2221.

Takeda, H. & Shimada, A. 2010. The art of medaka genetics and genomics: what makes them so unique? *Annu Rev Genet,* **44,** 217-241.

Tateishi, K., He, J., Taranova, O., Liang, G., D'alessio, A. C. & Zhang, Y. 2008. Generation of insulin-secreting islet-like clusters from human skin fibroblasts. *J Biol Chem,* **283,** 31601-31607.

Tehrani, Z. & Lin, S. 2011. Endocrine pancreas development in zebrafish. *Cell Cycle,* **10,** 3466-3472.

Teta, M., Long, S. Y., Wartschow, L. M., Rankin, M. M. & Kushner, J. A. 2005. Very slow turnover of beta-cells in aged adult mice. *Diabetes,* **54,** 2557-2567.

Tiso, N., Moro, E. & Argenton, F. 2009. Zebrafish pancreas development. *Mol Cell Endocrinol,* **312,** 24-30.

Upchurch, B. H., Aponte, G. W. & Leiter, A. B. 1994. Expression of peptide YY in all four islet cell types in the developing mouse pancreas suggests a common peptide YY-producing progenitor. *Development,* **120,** 245-252.

Wan, H., Korzh, S., Li, Z. et al. 2006. Analyses of pancreas development by generation of gfp transgenic zebrafish using an exocrine pancreas-specific elastaseA gene promoter. *Exp Cell Res,* **312,** 1526-1539.

Wierup, N., Svensson, H., Mulder, H. & Sundler, F. 2002. The ghrelin cell: a novel developmentally regulated islet cell in the human pancreas. *Regul Pept,* **107,** 63-69.

Willems, B., Büttner, A., Huysseune, A., Renn, J., Witten, P. E. & Winkler, C. 2012. Conditional ablation of osteoblasts in medaka. *Dev Biol,* **364,** 128-137.

Yee, N. S., Lorent, K. & Pack, M. 2005. Exocrine pancreas development in zebrafish. *Dev Biol,* **284,** 84-101.

Yesil, P. & Lammert, E. 2008. Islet dynamics: a glimpse at beta cell proliferation. *Histol Histopathol,* **23,** 883-895.

Zaret, K. S. & Grompe, M. 2008. Generation and regeneration of cells of the liver and pancreas. *Science,* **322,** 1490-1494.

Zecchin, E., Mavropoulos, A., Devos, N. et al. 2004. Evolutionary conserved role of ptf1a in the specification of exocrine pancreatic fates. *Dev Biol,* **268,** 174-184.

Acknowledgements

I would like to express my deepest and sincere gratitude to my supervisor, Dr. Hiroyuki Takeda (The University of Tokyo) for providing me with the opportunity to study in a splendid environment.

I would also like to express my sincere appreciation to Dr. Atsuko Shimada (The University of Tokyo) and Dr. Tatsuya Tsukahara (Harvard Medical School) for their support and discussion of my experiment; to Ms. Yasuko Ozawa, Ms. Yuki Yamagishi and Ms. Ikuko Fukuda for excellent fish care.

I am truly grateful to the members of Takeda laboratory (the Laboratory of Embryology, Department of Biological Sciences, Graduate School of Science, The University of Tokyo) for all they have done for my life in the laboratory.

Finally, I am greatly indebted to my family, Hiroshi, Junko, and Yuko Otsuka for their heartfelt support and generous affection, without which I would not have accomplished this study. I dedicate this doctoral thesis to them.